nature ecology & evolution

ARTICLES

https://doi.org/10.1038/s41559-020-01314-x

Nutritional niches reveal fundamental domestication trade-offs in fungus-farming ants

Jonathan Z. Shik[1,2,3]✉, Pepijn W. Kooij[2,4,9], David A. Donoso[5,6], Juan C. Santos[7], Ernesto B. Gomez[3], Mariana Franco[3], Antonin J. J. Crumière[1], Xavier Arnan[8,10], Jack Howe[2,11], William T. Wcislo[3] and Jacobus J. Boomsma[1,2]

During crop domestication, human farmers traded greater productivity for higher crop vulnerability outside specialized cultivation conditions. We found a similar domestication trade-off across the major co-evolutionary transitions in the farming systems of attine ants. First, the fundamental nutritional niches of cultivars narrowed over ~60 million years of naturally selected domestication, and laboratory experiments showed that ant farmers representing subsequent domestication stages strictly regulate protein harvest relative to cultivar fundamental nutritional niches. Second, ants with different farming systems differed in their abilities to harvest the resources that best matched the nutritional needs of their fungal cultivars. This was assessed by quantifying realized nutritional niches from analyses of items collected from the mandibles of laden ant foragers in the field. Third, extensive field collections suggest that among-colony genetic diversity of cultivars in small-scale farms may offer population-wide resilience benefits that species with large-scale farming colonies achieve by more elaborate and demanding practices to cultivate less diverse crops. Our results underscore that naturally selected farming systems have the potential to shed light on nutritional trade-offs that shaped the course of culturally evolved human farming.

Farming evolved by natural selection in several social insect lineages and as a cultural innovation in our human ancestors. Although analogies across these domains need to be phrased carefully, it is reasonable to assume that both types of farming became more sophisticated over time, which seems obvious from a crop perspective because our domesticated food plants often only remotely resemble their free-living ancestors. Over thousands of years, humans have continuously selected plant cultivars with nutritionally enhanced or enlarged leaves, roots, fruits and seeds[1,2], which facilitated modern agriculture's ecological expansion[3]. Domestication has also exposed production trade-offs as increasingly specialized crops came to rely on specific abiotic conditions that farmers needed to provide to match their cultivars' shrinking fundamental niches for moisture, temperature and nutrients[4]. Such trade-offs were especially pronounced when artificially selected traits ran counter to the naturally selected life histories that previously maximized fitness in wild cultivar ancestors confronting more hostile and fluctuating natural environments[5,6]. As domestication proceeded, culturally informed human farmers managed to push these trade-offs to extremes. For instance, crops in historically recent eras have been farmed across huge metapopulations even though their vulnerability to herbivores and pathogens has often increased[7], although the strength of such trade-offs can vary[8]. This geographic expansion has been enhanced by technological solutions that enable farmers to provide their crops with consistently optimized realized niches (for example, higher doses of pesticides).

The farming systems of ants[9,10], macrotermitine termites[11] and ambrosia beetles[10] required millions of years of natural selection to produce narrow mutualistic co-dependencies[12]. Rather than balancing nutritional needs by farming diverse foods as in large-scale human societies, these insect farmers, such as the fungus-farming attine ants that adopted agaricaceous fungal cultivars (order: Agaricales)[13,14], specialized on clonal monocultures of a limited suite of fungi. Despite this overall difference, ant farmers of diverse attine genera came to rear specialized cultivars with varying degrees of polyploidy[15] and basal metabolic rates[16] that appear to be linked to transitions to increasingly complex farming strategies. Throughout their shared co-evolutionary histories, fungus-farming ants also evolved specialized fungal enzyme recycling habits (to increase crop productivity)[17] and powerful antibiotic defences to control crop disease[18–21]. These fungicultural innovations have probably been instrumental in the ecological diversification and geographic expansion among the 19 extant attine genera encompassing >240 species that now inhabit most neotropical rainforests and many drier habitats from Argentina to the northeastern United States[22–25].

Given these historical domestication patterns, we hypothesized that: (1) ant farmers have solved a trade-off between crop yield and cultivar vulnerability; and (2) this trade-off hinges on nutrient availability as the core commodity of crop provisioning and yield. We used the nutritional geometry approach to test this hypothesis, capitalizing on its conceptual and empirical tools for visualizing and modelling trade-offs that organisms navigate to maintain nutritional homeostasis[26–29]. Our present study builds on an earlier one

[1]Section of Ecology and Evolution, Department of Biology, University of Copenhagen, Copenhagen, Denmark. [2]Centre for Social Evolution, Department of Biology, University of Copenhagen, Copenhagen, Denmark. [3]Smithsonian Tropical Research Institute, Panama City, Republic of Panama. [4]Comparative Fungal Biology, Department of Comparative Plant and Fungal Biology, Royal Botanic Gardens, Kew, London, UK. [5]Departamento de Biología, Escuela Politécnica Nacional, Quito, Ecuador. [6]Centro de Investigación de la Biodiversidad y Cambio Climático, Universidad Tecnológica Indoamérica, Quito, Ecuador. [7]Department of Biological Sciences, St. John's University, New York, NY, USA. [8]Centre de Recerca Ecològica i Aplicacions Forestals (CREAF), Cerdanyola del Vallès, Spain. [9]Present address: Center for the Study of Social Insects, São Paulo State University (UNESP), Rio Claro, Brazil. [10]Present address: Department of Biological Sciences, University of Pernambuco, Garanhuns, Brazil. [11]Present address: Department of Zoology, University of Oxford, Oxford, UK. ✉e-mail: jonathan.shik@bio.ku.dk

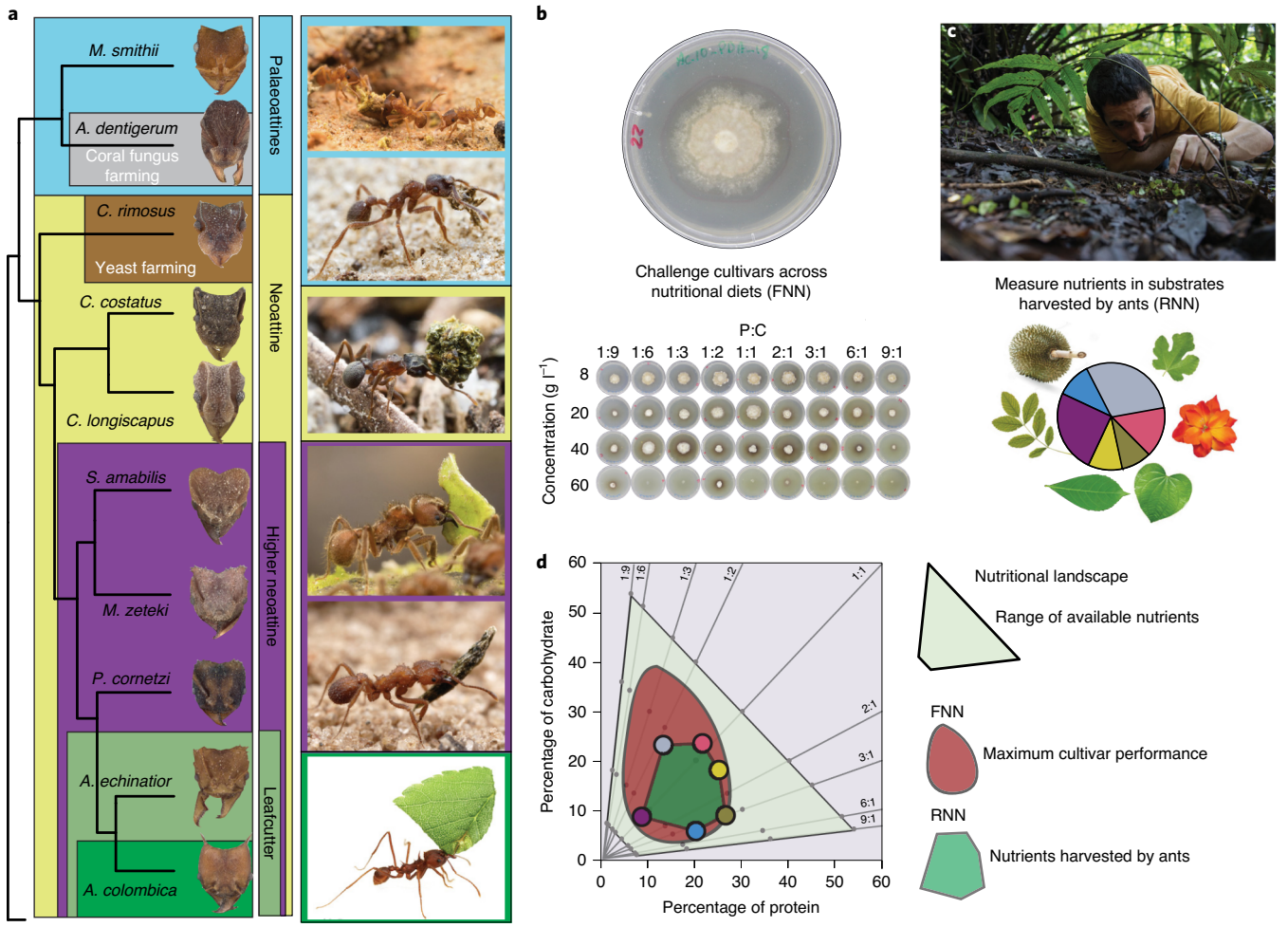

Fig. 1 | Assessment of domestication trade-offs across transitions in mutualistic farming practices of fungus-farming ants. a, Attine ants harvest a range of matter, from nutritionally variable detritus fragments in phylogenetically basal genera to freshly cut vegetation in the leafcutter ant crown group (the schematic phylogeny[21–23,34,35] is restricted to ten representative species co-occurring in Panama). The ants convert this crude forage into nutritional substrates for their fungal cultivars. Farming transitions included: Palaeoattines (*Mycocepurus* and *Apterostigma*) that have retained small colonies of 10–100 workers and include a clade within *Apterostigma* secondarily adopting a coral fungus cultivar; Neoattines (*Cyphomyrmex*) that cultivate fungi in a hyphal form and a lineage of yeast farmers; higher neoattines (*Sericomyrmex*, *Mycetomoellerius* and *Paratrachymyrmex*) that farm a fully domesticated single lineage of gongylidia-bearing cultivars; and leafcutters, including *Acromyrmex* (with up to thousands of workers per colony) and *Atta* (with up to millions of morphologically more specialized workers per colony). Where possible, we have used pictures of the same species represented in this study, but the *Mycetomoellerius* picture represents the closely related *M. tucumanus*[35], the *Apterostigma* picture is of an unknown species of that genus, the *Sericomyrmex* picture is of *S. mayri* and the *Atta* picture is of *A. cephalotes*. **b**, FNNs[29,31] of fungal cultivars are defined by quantifying their intrinsic tolerances and nutrient requirements after isolating cultivars from ant colonies and rearing them in vitro across substrates varying in concentrations and ratios of protein and carbohydrates (P:C). **c**, RNNs[29,31] (the macronutrients that ant farmers offer to their cultivars) are defined by sampling and nutritionally analysing substrates collected from the mandibles of returning attine foragers in the field. **d**, Nutrient provisioning strategies of farmers are assessed by overlaying substrate RNNs atop cultivar FNNs. Foraging ants can maximize cultivar performance with a substrate RNN nested inside their cultivar's FNN. In the example provided, the FNN (red bullseye) is derived from a nutritional landscape of 36 diets (small grey circles) spanning nine P:C ratios from 1:9 (carbohydrate biased) to 9:1 (protein biased) along which P:C ratios remain constant (grey lines extending from the origin) but total protein and carbohydrate concentrations increase. The RNN (green polygon) is bounded by nutritional blends of substrates collected by foraging ants in the field, shown here as coloured circles matching the substrates in the pie chart in **c**. Image credits: antweb.org (specimens in **a**), Alex Wild (https://www.alexanderwild.com/Ants) (foraging ants in **a**) and Sean Mattson (**c**).

in which we used nutritional geometry to quantify a related type of nutritional trade-off in the ant *Mycocepurus smithii*, a representative of the palaeoattine clade that is sister to the neoattines that evolved more organizationally complex farming systems. Colonies of *M. smithii* farm clones of a weakly domesticated fungal cultivar that can maximize the growth of edible hyphae in proportion to carbohydrate intake, but with the downside of encouraging cultivars to produce inedible mushrooms that may benefit fungal reproduction to the detriment of farmer fitness[30]. Here, we expand this nutritional geometry approach across the key evolutionary transitions towards higher organizational complexity in attine farming systems (Fig. 1a) by integrating their nutritional economy with ecological niche theory.

We tested the domestication trade-off between yield and vulnerability by performing a study with three objectives. The first was to quantify and visualize the breadth of fundamental nutritional niches (FNNs)[29,31] when fungal cultivars are grown in vitro across artificial nutritional landscapes varying in absolute and

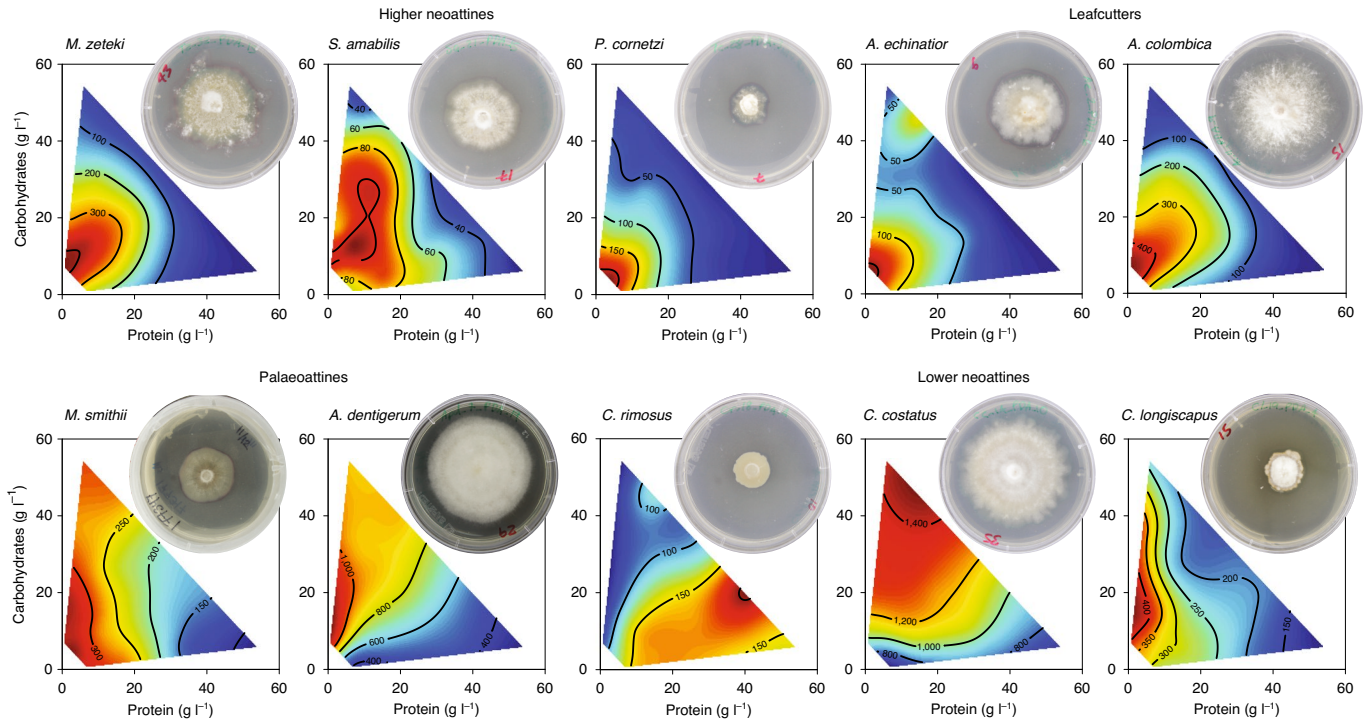

Fig. 2 | Heatmaps of cultivar growth used to describe cultivar FNNs. Bottom: diverse lower-attine cultivars with variable FNNs. Top: fully domesticated higher-neoattine cultivars with narrowed FNNs, showing maximum growth (red heatmap colour) on similar blends of protein and carbohydrates. Whereas dark blue heatmap values in the lower-attine plots indicate slower cultivar growth, dark blue values in the higher-neoattine and leafcutter plots often indicate cultivar mortality (see Extended Data Fig. 2). In each of the ten plots, cultivar growth (hyphal area (mm^2)) is visualized across 36 experimentally defined artificial media varying in absolute ($g\,l^{-1}$) amounts and relative (P:C ratio) amounts of protein and carbohydrates[30,67]. As illustrated in Fig. 1d, these substrates spanned nine P:C ratios (1:9, 1:6, 1:3, 1:2, 1:1, 2:1, 3:1, 6:1 and 9:1) and four protein + carbohydrate concentrations (8, 20, 40 and 60 $g\,l^{-1}$). We used the fields package[60] in R (ref. [61]) to visualize the response surfaces obtained from non-parametric thin-plate splines. The heatmaps show the average values of cultivars from three colonies (*A. dentigerum*, *C. costatus*, *P. cornetzi*, *A. echinatior* and *A. colombica*), two colonies (*M. zeteki* and *S. amabilis*) or one colony (*M. smithii*, *C. rimosus* and *C. longiscapus*). Inset images of petri dishes for each heatmap show an example of the specific cultivar's in vitro phenotype. FNNs for cultivar growth were consistent when measured across multiple colonies of an attine species, so we assume that the three single-colony estimates are representative (Extended Data Fig. 1). We used least-squares regressions to assess the underlying significance of linear and quadratic terms (and the linear interaction) across the 36 protein and carbohydrate substrate combinations and to validate the interpretation of FNN heatmaps of the dependent variables growth area (Supplementary Table 1) and percentage survival (Supplementary Table 2). All response surface regressions producing the heatmap colour gradients shown here were statistically significant (Supplementary Table 1).

relative abundance of protein and carbohydrate macronutrients (Fig. 1b). We used these results to interpret laboratory feeding experiments with nutritionally defined substrates that tested how ant farmers prioritize macronutrient intake within the performance constraints imposed by their cultivar's FNNs. Second, we examined whether and how ant farmers target their cultivar's nutritional niches while foraging across natural nutritional landscapes in the field (Fig. 1c). We quantified realized nutritional niches (RNNs)[29,31] of naturally collected substrates and assessed their nestedness within the experimentally obtained FNN dimensions of cultivars (Fig. 1d). Third, we assessed whether individual small-scale farming colonies within local populations can successfully maintain genetically different cultivars while foraging within a single nutritional landscape. We assessed whether small-scale farmers manage cultivar vulnerabilities differently compared with large-scale farmers achieving system resilience by cultivating uniform crops of low genetic diversity.

Results

Cultivar FNNs narrowed with full domestication but growth rates did not increase. First, we compared cultivar FNNs across three evolutionary stages of crop domestication[14] where we predicted that ant farmers solved the yield–vulnerability trade-off in different ways. We started with the palaeoattine genera *Mycocepurus* and *Apterostigma* and the genus *Cyphomyrmex*, which represents an early branch of the lower neoattines that would later produce the higher-neoattine genera described below (Fig. 1a). These three representatives probably resemble the ancestral fungus-farming attines that arose ~60 million years ago (Ma) because all retained small, low-productivity colonies of tens to hundreds of monomorphic workers and cultivars with undifferentiated hyphae to feed the ant farmers[14] (but see ref. [32] for a case of a differentiated cultivar). As expected, before full crop domestication, these cultivars exhibited broad FNNs with hyphal growth maximized across a wide range of protein:carbohydrate (P:C) ratios (Fig. 2 and Supplementary Table 1). These cultivar FNNs also varied widely among (but not within; Extended Data Fig. 1) cultivar types (Fig. 2), which probably reflects that these farmers have exchanged loosely domesticated fungi with free-living varieties over millions of years[33]. Despite this variation, the agaricaceous cultivars of *M. smithii* and *Cyphomyrmex costatus*, as well as the pterulaceous coral fungus *Myrmecopterula velohortorum* reared by *Apterostigma dentigerum*[34], all showed continuing or accelerated growth on carbohydrate-biased substrates at high nutritional concentrations (Fig. 2) relative to what can apparently be provided in detrital substrates collected by their ant farmers (see discussion of Fig. 4a below).

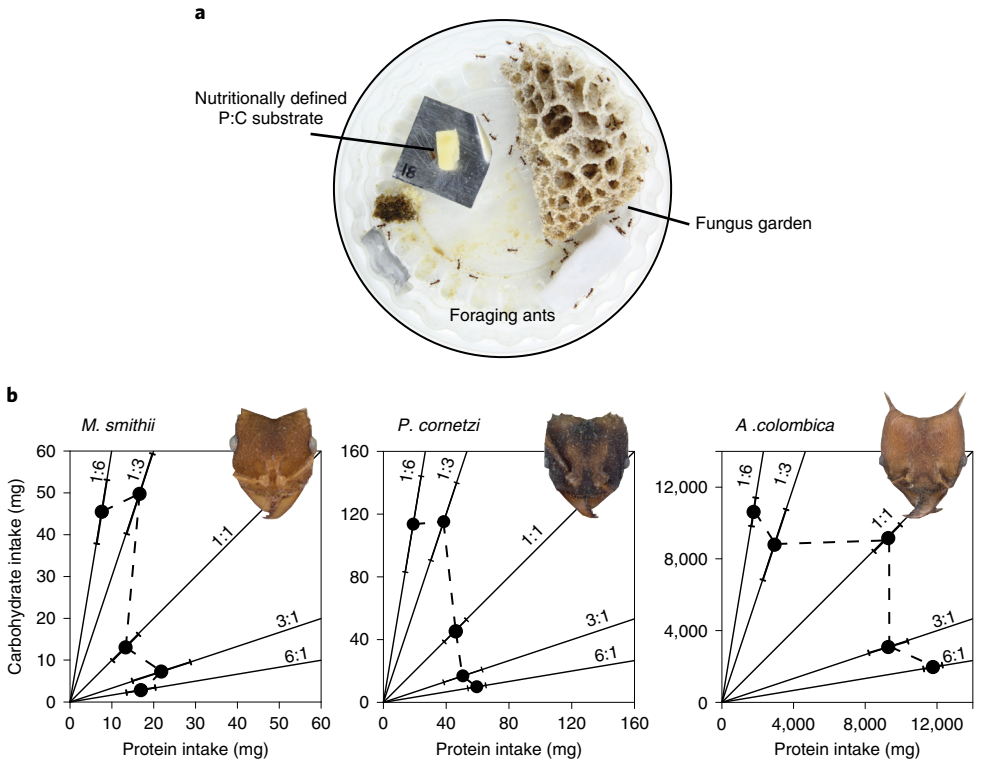

Fig. 3 | Laboratory experiments comparing foraging decisions of colonies of three representative attine ant species. A comparison of three species of attine ant showed that farming ants conform to their cultivar's FNN dimensions when allowed to forage on single nutritionally defined substrates. **a**, Representative image of an experimental colony of *P. cornetzi* during the laboratory feeding experiment. **b**, Intake levels show that colonies of *M. smithii* and *P. cornetzi* tightly regulated protein concentrations to remain at low levels while allowing carbohydrate levels to fluctuate widely across substrates. By contrast, colonies of *A. colombica* allowed for greater fluctuations of protein intake while sustaining high carbohydrate levels, even when restricted to the 1:1 P:C nutritional rail that *M. smithii* and *P. cornetzi* avoided (see also Extended Data Fig. 4). These no-choice feeding experiments were performed on laboratory-acclimatized colonies confined to single nutritional rails of agar-based substrates[68] (Supplementary Table 5) that constrained their intake to specific P:C ratios (1:6, 1:3, 1:1, 3:1 or 6:1)[26,30,69]. Dashed lines reflect decisions to over- or under-collect one macronutrient to avoid imbalanced intake of another limiting macronutrient. Mean substrate harvest values ± s.e. are presented coincident to intake rails[70]. We analysed cumulative intake rates over 15 d of feeding on these substrates (Supplementary Table 4). We present 15-d data for *P. cornetzi* and *M. smithii* to facilitate direct comparison with the *A. colombica* results, but the *P. cornetzi* experiment continued for 39 d, yielding long-term results that were consistent with the 15-d data (Supplementary Fig. 1 and Supplementary Table 4). The *M. smithii* experiment extended for 29 d and also yielded consistent results[30]. Colonies of *M. smithii* and *P. cornetzi* with collapsed fungus gardens were removed from the experiment on the day they had no remaining cultivar biomass left (Extended Data Fig. 5). Credit for ant specimen images in **b**: antweb.org.

Next, we measured the FNNs of cultivars in the higher-neoattine genera *Sericomyrmex*, *Mycetomoellerius* and *Paratrachymyrmex* (Fig. 1a), which evolved ~27–31 Ma[21,22,35]. The adaptive radiation of this clade coincided with the irreversible domestication of a specialized fungal lineage capable of concentrating nutrients in specialized swollen hyphal tips (gongylidia) bundled into staphylae[36–38]. The extant descendants of these higher neoattines represent an intermediate domestication phase characterized by farming fully domesticated cultivars but without changes in foraging substrates[39,40] and colony sizes[16,41] relative to the phylogenetically basal lower neoattines and palaeoattines. Consistent with their domesticated crops being derived from a single fungal ancestor, the cultivars of these higher-neoattine farmers had less variable FNNs than the palaeoattine and lower-neoattine cultivars, typically maximizing growth on substrates with 8–15 g l^{-1} protein and at rather low (8–25 g l^{-1}) absolute concentrations of carbohydrates (Fig. 2). The narrowed FNNs of these cultivars were confirmed because they often exhibited mortality in petri dish culture when they were provided with suboptimal nutrient mixtures (Extended Data Fig. 2 and Supplementary Table 2), consistent with expectations of the hypothesized domestication trade-off of specialization versus vulnerability.

The leafcutter ants represent the major expansion in scale and organizational complexity of neoattine fungus farming that appeared ~18.5 Ma[21,22] (Fig. 1a). The emergence of the leafcutter ants coincided with the use of freshly cut vegetation from hundreds of plant species[42] to provision massive gardens of the now obligately polyploid[15] staphylae-bearing cultivar *Leucoagaricus gongylophorus*[34] to support tens of thousands of ants in colonies of *Acromyrmex* and up to millions of individuals in colonies of *Atta*[24]. The performance responses of *L. gongylophorus* cultivars isolated from colonies of *Acromyrmex echinatior* and *Atta colombica* resembled those of the other higher-neoattine cultivars (Fig. 2 and Extended Data Fig. 1) and also often included steep mortality increases when confined to nutritional blends outside the cultivar's FNN (Extended Data Fig. 2). Thus, the P:C FNN of *L. gongylophorus* cultivars did not appear to have changed markedly in connection to the broader ecological niche of substrate provisioning displayed by the leafcutter ants[42].

The *L. gongylophorus* cultivar of leafcutter ants also exhibited statistically similar in vitro growth rates relative to cultivars of the other higher neoattines (Extended Data Fig. 3), which is remarkable because *Atta* foragers in the field provision cultivars with orders

of magnitude more substrate mass than any other attine genera[42]. In fact, cultivars of the smallest lower-attine colonies of *A. dentigerum* and *C. costatus* grew faster in vitro on a standard potato dextrose agar (PDA) medium known to generally promote high cultivar growth rates[25,43] than all other cultivars tested (Extended Data Fig. 3). This result appears to be analogous to the minor changes in growth rate of plant crops during and after human domestication[7] and suggests that accelerated intrinsic cultivar growth rates neither drove nor responded to later increases in the scale and organizational complexity of fungus farming in neoattine ants.

Foraging ants collect nutrients within the FNN dimensions of their cultivars. Ant and human farmers nutritionally provision their cultivars in fundamentally different ways. While humans farm mostly autotrophic plants that need targeted blends of inorganic NPK fertilizers, attine ant farmers maintain heterotrophic fungi that need organic inputs in the form of freshly cut plant material, or scavenged insect frass and other detritus that foragers must gather from their environment (Fig. 1). Fungal cultivars also have no independent resource acquisition via roots, so the ants need to provide crops with almost all of their nutrients as crude forage[44]. These chemically and physically complex substrates contain the required protein and carbohydrate macronutrients, but also water, micronutrients and vitamins, toxins and recalcitrant cell wall fibres[37,45]. We used nutritional geometry tools to cut through this complexity and explore whether and how in vitro measures of cultivar FNN breadth in terms of two macronutrients constrain the nutritional content of substrates collected by the fungus-farming ants when they forage.

We performed laboratory feeding experiments to measure nutrient regulation strategies in attine colonies confined to single nutritionally defined substrates with varying P:C ratios (Fig. 3a). For these experiments, we focused on comparing three attine species representing the main domestication transitions described above: palaeoattines (*M. smithii*), higher neoattines (*Paratrachymyrmex cornetzi*) and crown-group neoattine leafcutters (*A. colombica*). We found that the leafcutter ants targeted broader protein dimensions than the two other species (Fig. 3b). Specifically, *A. colombica* foragers collected more of the protein-rich 1:1 P:C substrate than both *M. smithii* and *P. cornetzi*, which tightly regulated protein intake to remain at low levels across all P:C substrates (Fig. 3b, Extended Data Fig. 4 and Supplementary Table 4). Colonies of *P. cornetzi* and *M. smithii* also had an aversion to substrates with macronutrient ratios above 1:3 P:C, possibly because these blends are associated with increased risks of crop failure (Extended Data Fig. 5) and worker mortality (Supplementary Fig. 2a) and reduced total colony biomass (Supplementary Fig. 3a) for both *P. cornetzi* (Supplementary Table 6) and *M. smithii*[30]. The tight regulation of protein intake by foragers of these two species matched the narrow in vitro protein FNNs of their cultivars (that is, the steep declines in growth beyond 15 g l^{-1} protein; Fig. 2).

The leafcutter ants did not face a similarly extreme vulnerability–yield trade-off between starving fungal cultivars of carbohydrates or over-harvesting protein when confined to nutritionally imbalanced substrates (Fig. 3b, Extended Data Fig. 4 and Supplementary Table 4). In fact, *A. colombica* colonies showed greater stability across all P:C substrates tested, remaining stable or increasing in both worker numbers (Supplementary Fig. 2b and Supplementary Table 6) and colony mass (Supplementary Fig. 3b and Supplementary Table 6). Yet, *A. colombica* colonies also appeared to walk a nutritional tightrope since their foraging levels also varied with substrate macronutrient ratios. Specifically, *A. colombica* workers collected significantly smaller amounts of carbohydrates when confined to the most protein-biased substrates (3:1 and 6:1 P:C diet treatments; Extended Data Fig. 4). Thus, while *A. colombica* colonies maintained relatively high foraging levels under these protein-biased conditions (Fig. 3b), they still experienced carbohydrate shortfall relative to levels that could maximize cultivar growth on carbohydrate-biased diets. This may be related to the steep in vitro decline in growth (Fig. 2) and survival (Extended Data Fig. 2) exhibited by *L. gongylophorus* beyond substrate protein concentrations of 30 g l^{-1}—a level that resembled (but was slightly higher than) that for the cultivars of *P. cornetzi* that we tested.

Quantifying the RNN dimensions of foraging ant farmers in the field. The targeting of FNNs that maximize hyphal growth (Fig. 2) while avoiding inedible mushroom production is a documented nutrient-mediated trade-off that occurred before attine ants fully domesticated their cultivars[30]. However, mushrooms were never produced by plated cultivars of neoattine ants, so we expected them to exhibit more subtle domestication trade-offs. Analogous to human crops that no longer exchange genes with wild or feral relatives, higher-neoattine ant farmers are expected to nutritionally provision their cultivars to optimize resource allocation between somatic hyphal growth and the fraction of this growth to be harvested as

Fig. 4 | Fungus-farming ants representing different stages of cultivar domestication and organizational complexity navigate nutritional landscapes to harvest RNNs relative to their cultivar's FNNs. Lying down on the forest floor next to nest entrances, we collected and catalogued tiny substrate bits from the mandibles of laden workers returning to their colonies. Individual substrate types are represented by coloured wedges in the pie charts (left), corresponding to the coloured circles in the RNN maps (middle and right) (see Fig. 1c,d). Middle plots show hyphal area (mm^2) illustrated with an inset outlined image of the specific fungus grown on a petri dish, whereas right plots show the percentage of plates producing mushrooms illustrated by inset petri dish image of the mushroom phenotype (**a**) or staphyla density per mm^2 illustrated by magnified schematic view of staphyla on fungi grown on petri dishes (**b** and **c**). **a**, The palaeoattine ant *M. smithii* collected 52% insect frass, 29% wood pieces, 14% small seeds, 2% flowers and 3% other undefined bits of detritus in terms of the proportion of sampled substrate biomass (26.3 mg dry mass in total from 20.5 h of collection)[30] (Supplementary Table 7). This yielded an RNN enabling the ants to provision cultivars with 0.6–25.8% TNCs while also enabling 0.1–27.0% protein (Supplementary Table 9). **b**, The higher-neoattine ant *P. cornetzi* rears a fully domesticated gongylidia-bearing cultivar, but colonies continue to forage like lower-attine ants, collecting detritus (60.1% insect frass, 10.7% detrital leaf fragments, 9.2% seeds, 3.5% flower pieces, 3.3% wood bits and 13.1% other; 225 mg dry mass in total from 43.7 h of collection; Supplementary Table 7). These substrates yielded an RNN with similar dimensions as harvested by *M. smithii*, with 0.6–25.8% TNCs and 0.1–30.84% crude protein (Supplementary Table 9). **c**, The leafcutter ant *A. colombica* has a different foraging strategy of primary herbivory, focusing on fresh leaves that foragers cut from many plant species (here represented by 13 different vegetative substrates harvested by a single colony; 40,026 mg dry mass in total from 9 h of collection; Supplementary Table 8). These substrates range widely in both the percentage of TNCs (7.47–33.76%) and crude protein (4.64–34.83%; Supplementary Table 8). Capturing the macronutrient range of different substrate types collected by *M. smithii* and *P. cornetzi* required larger pooled samples of similar substrates collected from leaf litter traps and flower petal samples collected from the mandibles of *A. colombica* that resembled those foraged by *M. smithii* and *P. cornetzi*. Details about sampling and nutritional analyses are provided in the Methods and Supplementary Tables 7–9. The slightly larger white areas in the low-concentration nutrient space (lower-left corners) of these fungal FNN heatmaps relative to their representations in Fig. 2 resulted from the conversion of macronutrient units of g l^{-1} to percentage of dry diet mass within in vitro diet recipes. This facilitated comparison of cultivar FNNs and substrate RNNs and did not impact the interpretation of the results. The regressions underlying variation in growth area and staphyla density across P:C substrates for the fungal FNN plots were significant (Supplementary Tables 1 and 10).

edible staphylae with gongylidia. We therefore tested whether and how ant farmers in the field resolved nutrient provisioning vulnerabilities in their crops by estimating colony-level RNNs that could be mapped on the specific FNN dimensions obtained by rearing cultivars in vitro.

As before, we compared three attine species representing the transitions from the collection of mostly frass (leaf material processed through the guts of insect herbivores; secondary herbivory) in *M. smithii* and *P. cornetzi* and freshly cut vegetation in *A. colombica* (primary herbivory). To assess RNNs, we collected, weighed and catalogued samples of substrates collected from the mandibles of laden foragers as they returned to their nests, representing 77 h of total field observations from 22 colonies of *M. smithii* (Supplementary Table 7), 44 colonies of *P. cornetzi* (Supplementary Table 7) and one colony of *A. colombica* (Supplementary Table 8). We then nutritionally analysed substrates collected by foragers from the same study populations, representing 19 colonies of *M. smithii*, 33 colonies of *P. cornetzi* (Supplementary Table 9) and one colony of *A. colombica* (Supplementary Table 8).

We expected colonies of each ant species to forage for natural substrates within the range of experimentally obtained FNNs of their cultivars (that is, that their RNNs would not exceed their cultivars' upper physiological tolerances and would tend to converge on the performance-maximizing dimensions (dark red)

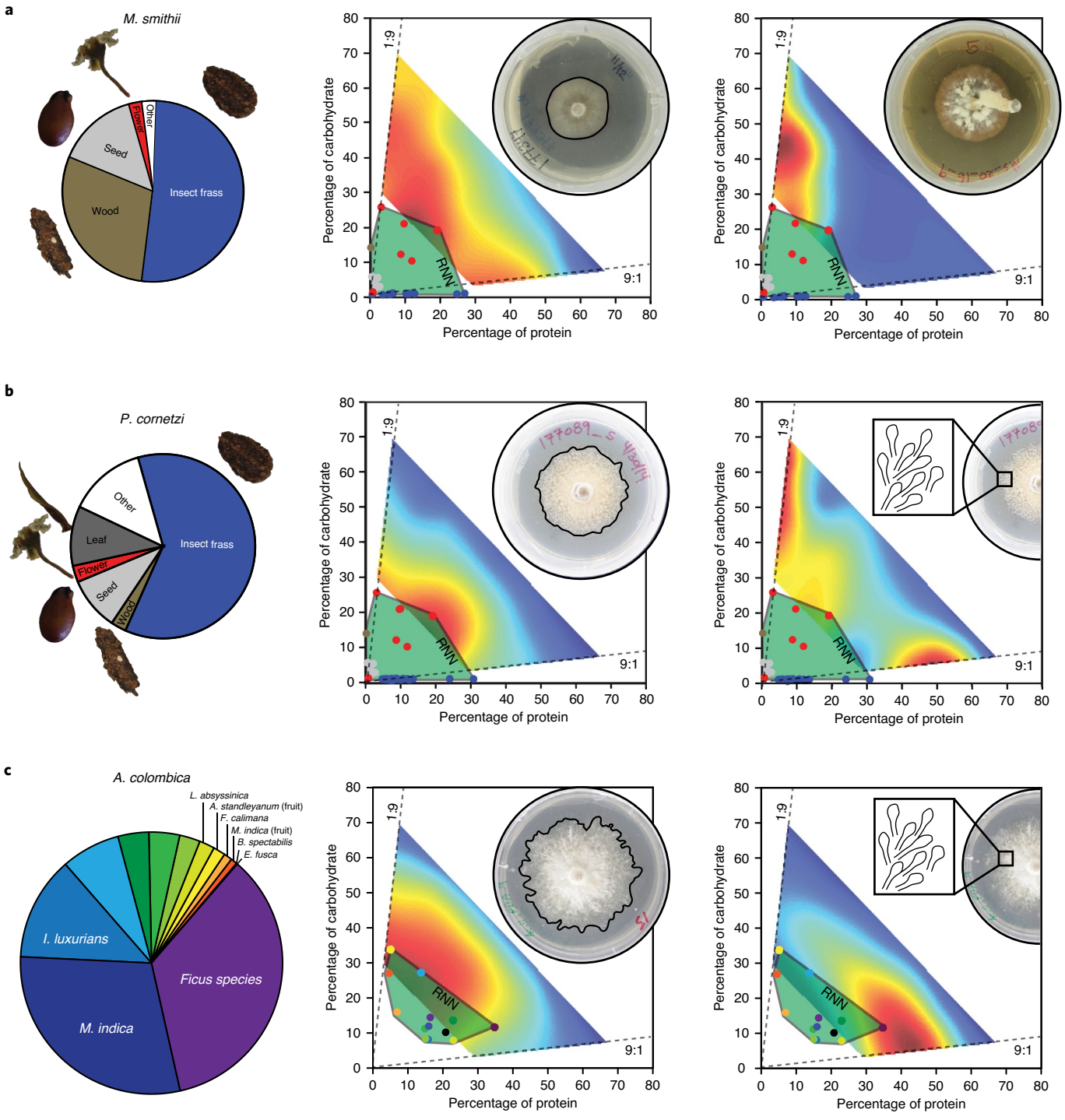

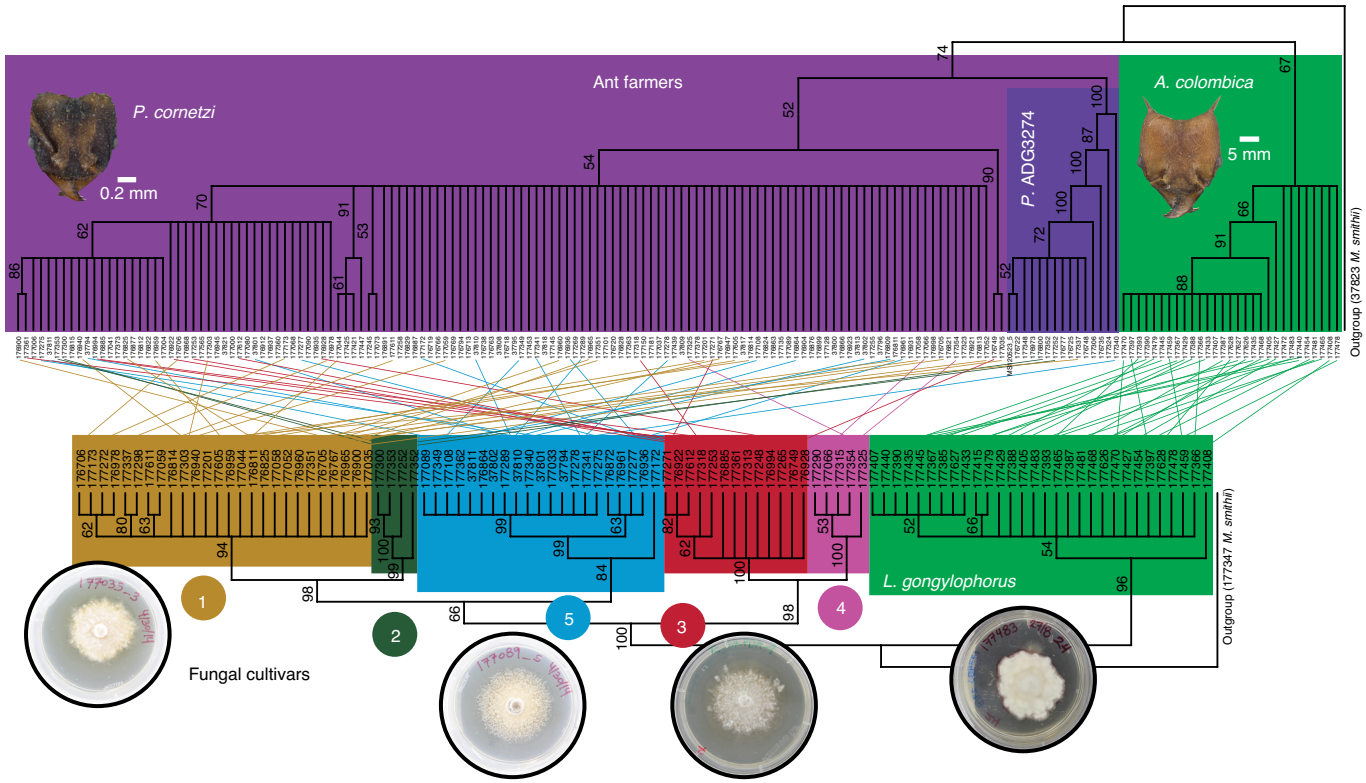

Fig. 5 | Comparison of two fully domesticated farming systems with different operational scales and ecological impacts. Within Soberanía National Park, the higher-neoattine ant *P. cornetzi* cultivates five haplotypes of related *Leucoagaricus* fungi with bootstrap support indicating that each of the five coloured cultivar clades represents a separate fungal haplotype. Each of these fungal haplotypes was also widely distributed across Soberanía National Park (Extended Data Fig. 9) and probably across the neotropics[35]. By contrast, the leafcutter ant *A. colombica* farms only a single cultivar species, *L. gongylophorus*. The bootstrap majority consensus barcoding tree based on the cytochrome *c* oxidase I (*CO1*) gene for the ants indicated that Panamanian *P. cornetzi* includes a morphologically cryptic species (hereafter, *P.* ADG3274) that farms an overlapping diversity encompassing at least three of the five *P. cornetzi* cultivars. The status of *P.* ADG3274 as a distinct cryptic species was supported by microsatellite analyses (Extended Data Fig. 7) and additional barcoding showing that while *P.* ADG3274 was relatively uncommon at our study site it has a regional distribution extending at least to Costa Rica (Extended Data Fig. 8). We do not further consider *P.* ADG3274 in the present study. The bootstrap majority consensus tree for ants is based on a section of the *CO1* gene of ~1,100 bp and includes 130 colonies of *P. cornetzi*, 15 colonies of *P.* ADG3274 and 29 colonies of *A. colombica* (Supplementary Table 13). The bootstrap majority consensus tree for fungi is based on a section of the LSU gene of ~820 bp and a section of the ITS marker of ~550 bp, and includes samples from 69 colonies of *P. cornetzi* and *P.* ADG3274 (fungal haplotypes 1 ($n=26$), 2 ($n=4$), 3 ($n=13$), 4 ($n=5$) and 5 ($n=21$)) and 29 colonies of *A. colombica* (Supplementary Table 14). Both ant and cultivar trees were rooted with an *M. smithii* ant or fungus sample. Credit for ant specimen images: antweb.org.

of the nutritional FNNs (Fig. 1c,d). We first found that foragers of *M. smithii* harvested sufficient amounts of protein (horizontal axis) to be able to avoid the cultivar FNN region that would produce inedible mushrooms, matching previous results[30]. However, while these detrital substrates provided a minimal protein level, they were also below the higher carbohydrate concentrations (vertical axis) that could accelerate cultivar growth (Fig. 4a). Second, colonies of *P. cornetzi* harvested substrates that yielded an RNN whose protein and carbohydrate amounts fell somewhat below the FNN regions maximizing both growth and staphyla density (Fig. 4b) while avoiding the high-concentration nutritional blends that induced cultivar mortality in vitro (Extended Data Fig. 2). Third, the representative *Atta* leafcutter ant colony achieved a comparatively broader RNN with higher maximum concentrations of macronutrients (Fig. 4c). This enlarged leafcutter RNN spanned the distinct FNN peaks for hyphal growth and staphyla production.

Cultivars with variable FNNs co-exist in a single nutritional provisioning environment. Many attine ant species maintain mutualistic associations with several fungal haplotypes[46–48]. This trait also applies to human farming but is puzzling in attine farms that are constrained to rearing a single cultivar clone that is usually vertically acquired[12,49]. For instance, if neighbouring colonies of the same ant species farm genetically distinct cultivars with different FNNs, one should expect considerable farmer plasticity to target RNNs that match their cultivar's specific needs. To assess the extent of performance variation across cultivars, we compared two attine species with different levels of fully domesticated crop specificity: (1) the leafcutter ant *A. colombica* as a single ant species (Extended Data Fig. 6) that farms a single species of *L. gongylophorus* cultivar (Fig. 5); and (2) the higher neoattine *P. cornetzi* (Fig. 5 and Extended Data Figs. 7 and 8) known to farm one of several possible species of fungal cultivar across our study area in Panama[48].

P. cornetzi farmed five cultivar haplotypes (Fig. 5) with similar FNNs for hyphal growth that also roughly matched those of the *L. gongylophorus* cultivar of *A. colombica* (Fig. 6a) and were consistent with other fully domesticated higher-neoattine cultivars tested (Fig. 2). However, the FNNs for staphyla density among isolates of the single cultivar species of *A. colombica* were much more consistent than the FNNs of the different cultivar haplotypes reared by *P. cornetzi* (Fig. 6a). In particular, the staphyla density FNN of cultivar haplotype 1 was similar to the FNN of *L. gongylophorus* reared

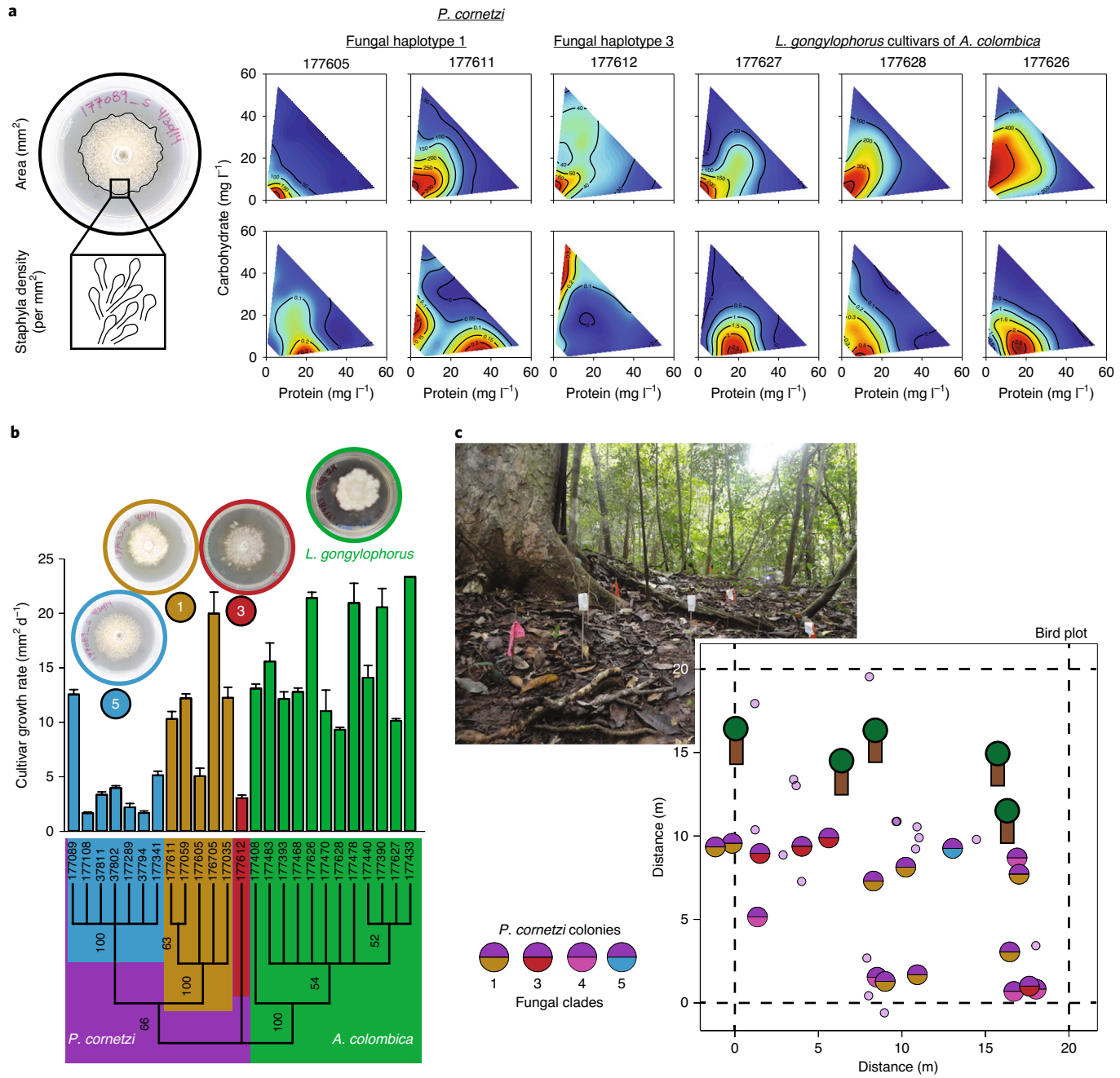

Fig. 6 | Colonies of *P. cornetzi* co-exist within nutritional foraging environments despite farming different cultivar haplotypes with variable properties of nutrient yield and growth. a, Fungal cultivars of *P. cornetzi* and *A. colombica* exhibited similar FNNs for maximum hyphal growth (top row). However, *P. cornetzi* (fungal haplotypes 1 and 3) had more variable FNNs for staphyla density (bottom row) while differences across these performance variables were much less variable for the *L. gongylophorus* cultivars of *A. colombica*. All response surface regressions for fungal growth area (Supplementary Table 1) and staphyla density (Supplementary Table 10) were significant, supporting the interpretation of their response contours. **b**, Testing three of the cultivar haplotypes isolated from 13 *P. cornetzi* colonies against *L. gongylophorus* cultivars from 12 *Atta* colonies showed that the former grows slower and with greater variation (means + s.e. of mycelial area per day of growth) on in vitro standardized PDA media than the *A. colombica* cultivars ($F_{1,22} = 12.76$; $P = 0.002$). Visual inspection of the growth results plotted on the phylogeny further suggested strain-specific variation in the mean cultivar growth rate, although additional sampling will be needed to provide sufficient statistical power for phylogenetically explicit analyses. Haplotype numbers are shown in coloured circles. **c**, *P. cornetzi* ants farm diverse fungal cultivar haplotypes in sympatry, with four of the five identified cultivars co-occurring within a single 20 m² monitoring plot within Soberanía National Park (Extended Data Fig. 9). Thus, colonies separated by <1 m often farm different cultivar haplotypes. Our estimates of local cultivar richness in this example plot are conservative as we sequenced fungal cultivars from a subset of 18 (larger purple semi-circles) of the 35 *P. cornetzi* colonies that we mapped over 23 searching hours. The small light purple circles indicate *P. cornetzi* colonies where only the ants were genotyped, and the stylized tree symbols indicate trees with a diameter at breast height of >1 m.

by *A. colombica* and protein biased (from 3:1 to 9:1 P:C) at intermediate nutrient concentrations (20 g l^{-1}) (Fig. 6a), while the staphyla density FNN for cultivar haplotype 3 of *P. cornetzi* was carbohydrate biased (1:9 P:C) at high nutrient concentrations (40–60 g l^{-1}). This cultivar variation extended to intrinsic growth rates viewed across the distinct cultivar haplotypes farmed by *P. cornetzi* (Fig. 6b),

although further sampling will be needed to confirm this apparent phylogenetic variation.

Variable FNNs for maximum staphylae density raise questions about the plasticity required by small-scale *P. cornetzi* farmers who found colonies with one specific crop symbiont and are unable to predict what mixture of forage items their habitat patch will provide over time. Such variability may help to explain why colonies primarily balance their foraging between two main detrital resources (that is, frass (variable in protein and low in carbohydrates) and wood chips (variable in carbohydrates and low in protein)) while also targeting nutritionally variable bits of plant material that also have a higher total concentration of both (for example, flowers, seeds and detrital leaf bits) (Fig. 4b and Supplementary Table 7). Further research will be required to resolve whether *P. cornetzi* colonies are actually able to dynamically adjust the cumulative sum of these alternative resources to enable them to achieve their optimum RNN under most circumstances.

The need for plasticity in cultivar provisioning also became apparent after we mapped spatial colony distributions across higher-neoattine species within our 20 m^2 leaf litter plots. This showed that *P. cornetzi* is part of a diverse assemblage of similarly sized higher-neoattine (non-leafcutter) farming species (*Paratrachymyrmex*, *Mycetomoellerius* and *Sericomyrmex*) in Soberanía Park (Extended Data Figs. 7 and 8), with colonies of four to seven species (mean ± s.d.: 5 ± 1) co-existing in close sympatry and at high densities of 21–66 colonies (mean ± s.d.: 43 ± 17) per 20 m^2 plot. *P. cornetzi* was the most abundant of these farming ant species with 20 ± 13 (range 4–35) colonies per 20 m^2 (Fig. 6c and Extended Data Fig. 10). At a community scale, most of these fungus-farming ant species share at least some symbionts[48] so that neighbouring colonies separated by <1 m are within each other's foraging range. Different fungal haplotypes with potentially different physiological needs thus co-exist within a single local nutritional environment.

Discussion

Towards an ecological explanation of the history and current impact of ant farming. Quantifying nutritional niches of fungus-farming ants reveals a domestication trade-off between vulnerability and yield. First, weakly domesticated palaeoattine and lower-neoattine cultivars tend to express generalist traits reminiscent of free-living fungi. These include broad and variable FNNs that probably match ecological conditions found in nutritional landscapes available outside regulated nest environments. For instance, their high growth rates at high nutrient concentrations appear to exceed nutrients available from ant detritus provisioning, and may instead reflect an ability to exploit ephemeral pulses of leaf litter resources[50]. Second, fully domesticated cultivars of higher-neoattine and leafcutter ants express similarly narrowed FNNs, probably reflecting that they are derived from a single fully domesticated *Leucoagaricus* ancestor. The trends observed across attine species generally match the expectations of a domestication trade-off where increased productivity through specialized nutritional yield benefits (that is, staphylae with gongylidia) in a narrowed suite of environmental conditions coincide with an increasingly remote resemblance to the cultivar traits that characterized the ancestral free-living fungi.

Our results reveal only minor expansions in FNN breadth of the specialized *L. gongylophorus* cultivar of leafcutter ants compared with the genetically more variable but likewise fully domesticated cultivars of *P. cornetzi*. This result seems surprising at first because leafcutter ants are remarkably generalist foragers that collect fresh leaves and flowers from hundreds of plant species[42]. However, the broad RNN dimensions of *Atta* colonies that we recorded in the field (Fig. 4c) were consistent with higher degrees of symbiotic resilience when we exposed colonies to nutritionally imbalanced substrates in laboratory experiments (Fig. 3). Moreover, leafcutter ant workers have evolved many specialized traits enhancing farming performance[18–20,51–53]. Specialized gardener castes may thus help to secondarily adjust the harvested substrates relative to required RNN dimensions when they macerate leaf fragments into a leaf pulp mixed with glandular and faecal fluids[17–19]. A suite of bacterial symbionts was also recently discovered in leafcutter ant digestive tracts[54] and fungus gardens[55] that may help to maintain the wide RNN of *Atta* leafcutter ants by providing nitrogen fixation services[55], by recycling excess amino acids such as arginine, or by converting plant-sap citrate into acetate to directly fuel ant metabolism[40].

A range of nutritional solutions to a fundamental domestication trade-off. Our study focused on three representative attine ant model species varying in colony size and scale of farming, to explore: (1) the unique cultivation challenges and opportunities each symbiosis faces; and (2) how each farming system maximizes cultivar performance by mixing nutritionally variable substrates collected from the environment. Our results highlight that there is no single answer to how fungus-farming ants navigate the complex nutritional landscape of a tropical rainforest to target RNNs within the FNNs of their specific cultivars to maximize edible yield. Since the cultivars of palaeoattines deliver undifferentiated hyphae as food, *M. smithii* ants need only to mix in sufficient protein via frass provisioning to avoid wasteful mushroom production, which is achievable but probably precludes rapid garden growth[30]. The two more complex farming systems have a differentiated cultivar so that the maximization of crop growth (hyphal mass) and edible harvest (staphyla density) have become separate optimization challenges. In the higher neoattine *P. cornetzi*, opportunities for maximizing yield appear to be somewhat constrained by the nutritional FNN targets that may vary across cultivar haplotypes (Fig. 6a). Some farmers may thus maximize edible yield by collecting more flower petals to acquire extra carbohydrates, while others may benefit from the additional protein available in frass. To detect such dynamic nutritional provisioning strategies, longitudinal sampling of individual colonies will be useful for describing how RNNs change over time, and broader sampling of colonies across habitat types will help determine the resiliency of RNNs among colonies with access to different suites of nutritionally variable substrates.

Our results further showed that the detrital substrates collected by palaeoattine and non-leafcutter neoattine ants tend to be nutrient-poor resources, so that farming productivity is likely to be ecologically constrained because their cultivar FNNs peak at higher nutrient concentrations than the ants can usually provide. The expanded RNN of *Atta* leafcutter ants provisions a highly specialized cultivar and appears to have partially overcome such constraints by being able to handle both more diverse macronutrient mixtures and higher absolute macronutrient quantities. The *Atta* cultivar also appeared to be special because it offers the farming ants two distinct macronutrient performance targets: one for hyphal growth (a carbohydrate-biased FNN) and one for staphyla density (a protein-biased FNN). Thus, our results suggest that the RNN expansion achieved by *Atta* leafcutter ants may have allowed a novel form of farming flexibility that could capitalize on high-quality (protein-rich) substrates when available without simultaneously enhancing cultivar growth rate per se.

We expect that future work will elaborate on the ecological pathways of fungal cultivar domestication by focusing on nutritional aspects of: (1) the earliest domestication trade-off at the origin of attine fungus farming between the yield of incipient crops and the costs of abandoning hunter-gathering[16,56]; (2) the diversification of farming practices across habitats and biomes[57] as attine lineages diverged and adapted to very different plant substrates[14,22]; and (3) the challenges of maintaining farming homeostasis in response to stochastic environmental variation[25], particularly in large-scale

farming systems that evolved quite differently in *Acromyrmex* and *Atta* leafcutter ants. Further progress in answering questions of this kind is feasible because the attine ants are the only insect farming clade where many farming systems varying widely in scale and organizational complexity co-exist within the same ecosystems. This contrasts with the large-scale agricultural systems of humans that have tended to competitively displace subsistence farms in many habitats[58], with the fungus-farming termites where only more organizationally complex forms of agriculture exist[11] and with the ambrosia beetles that invariably remained small-family cooperative breeders in tunnels that colony foundresses need to excavate in host trees[59].

Methods

Study populations. All attine colonies were harvested from the lowland tropical rainforest at Soberanía National Park, Panama (9.13528° N, 79.72141° W) from 28 October 2013 to 10 June 2015, with additional fieldwork conducted from 1 May to 30 June 2019. We located nest entrances of palaeoattines, lower neoattines and higher neoattines under leaf litter by placing polenta bait on the ground and following laden workers back to their nests. Leafcutter nests were visible as large established colonies and small dirt mounds of recently founded colonies. Back in the laboratory at the Smithsonian Tropical Research Institute (STRI) in Gamboa, we established colonies (see Supplementary Table 5 for demography) in plastic containers with ad lib water and ground polenta (or leaves for *Atta*), and acclimatized them to laboratory conditions at 24 °C. Ant vouchers were stored at STRI in Panama and fungal vouchers used in barcoding analyses were stored at Kew Gardens in the United Kingdom.

Estimating ant cultivar FNNs and their growth performance in vitro. We isolated fungus from 51 colonies of ten attine species, including *M. smithii* (ten colonies), *A. dentigerum* (three), *Cyphomyrmex rimosus* (one), *C. costatus* (three), *Cyphomyrmex longiscapus* (one), *P. cornetzi* (13), *Mycetomoellerius zeteki* (two), *Sericomyrmex amabilis* (two), *A. echinatior* (three) and *A. colombica* (13) (Supplementary Table 3). We grew these fungal cultivars on sealed sterile petri dishes containing PDA media (Difco) and used them to generate pure fungal stock cultures. We then used PDA as a standard medium to compare cultivar growth rates[25,43], placing 19.6 mm² cylindrical plugs of pure culture into separate 60 mm × 15 mm petri dishes containing 15 ml PDA. To estimate these intrinsic growth rates, we photographed the plates every 10 d for periods of 25–76 d (depending on the overall growth rate of the cultivar; Supplementary Table 3) and then used ImageJ (NIH Image; version 1.49) to measure the cumulative fungal growth after 30 d (area mm²).

We visualized the FNNs of cultivar fungi isolated from nests of ten attine species ($n = 22$ colonies), including *M. smithii* (one), *A. dentigerum* (three), *C. rimosus* (one), *C. costatus* (three), *C. longiscapus* (one), *P. cornetzi* (three), *M. zeteki* (two), *S. amabilis* (two), *A. echinatior* (three) and *A. colombica* (three) (Supplementary Table 3). We inoculated fungi in petri dishes containing 12 ml of 36 sterile synthetic agar-based substrate treatments varying in P:C (1:9, 1:6, 1:3, 1:2, 1:1, 2:1, 3:1, 6:1 or 9:1) and P + C concentration (8, 20, 40 or 60 g l^{-1}) ($n = 8$ plates per substrate × 36 dilution treatments = $n = 288$ plates per colony; $n = 6{,}336$ plates). We used growth rates on standard PDA media to set the length of P:C growth experiments for each cultivar (Supplementary Table 3).

Nutritionally defined media that were used to quantify cultivars' FNNs included distilled water and bacteriological agar (1.6% wt:vol; Amresco), carbohydrates as equal parts sucrose (Doradita cane sugar) and starch (from potato; Sigma–Aldrich), protein as equal parts bacto peptone (enzymatic digest of protein; BD), trypticase peptone (pancreatic digest of casein; BD) and bacto tryptone (pancreatic digest of casein; BD). We also included a crushed multivitamin mixture (Centrum) at a concentration of 2% of the mass of protein + carbohydrates (see ref. [30] for recipes). These ingredients were mixed with 200 ml distilled water on a stirring plate for 5 min and then sterilized by autoclaving at 121 °C, yielding a pH of 6.9.

We mapped fungal growth areas across the 36-substrate arrays using the fields package[60] in R (version 3.2.4)[61]. We plotted nutritional landscape contours using non-parametric thin-plate splines and set the topological resolution of response surfaces to $\lambda = 0.001$ as a smoothing parameter. We then used least-square regressions to assess the underlying significance of both linear and quadratic terms (and their interactions) and to verify the interpretation of FNN heatmaps based on fungal growth areas across the 36 protein and carbohydrate substrate combinations. Unless otherwise noted, we present heatmaps based on means of cultivars farmed by each attine species, but also provide all additional heatmaps for individual cultivars sampled from each attine colony in Fig. 6a (*P. cornetzi* and *A. colombica*) and Extended Data Fig. 1 (all other colonies), as well as the underlying statistical analyses (Supplementary Tables 1 and 10).

Each of the higher-neoattine and leafcutter cultivar haplotypes that we tested exhibited mortality on a subset of P:C substrates outside the range of the FNN. Mortality was indicated by inoculation plugs being clear (empty of fungus) or by lack of growth from the inoculation plug onto the P:C substrate by the end of the experiment (Extended Data Fig. 2). We generated heatmaps as described before ($\lambda = 0.01$ for the percentage data), with survivorship averaged across cultivars isolated from nests of a given attine species, standardizing the heatmap colour scale from 0–100% survival. We statistically assessed the significance of underlying regressions as described for the growth area heatmaps. This type of mortality response was never observed in the palaeoattine or lower-neoattine cultivars tested.

Laboratory no-choice feeding experiments with ant colonies and their natural cultivars. We analysed nutrient regulation strategies of laboratory-acclimatized colonies using nutritional geometry feeding experiments based on agar-based mixtures of protein and carbohydrate macronutrients (1.6 g agar per litre) at P:C ratios of 1:6, 1:3, 1:1, 3:1 and 6:1, and protein + carbohydrate dilutions of 100 g l^{-1} (for *P. cornetzi* and *A. colombica*) (Supplementary Table 11) or 20 g l^{-1} (for *M. smithii*)[30]. To evaluate evolutionary trends across a broader dataset than the one collected for the present study, we included some previously published data from a parallel study we performed on *M. smithii*[30]. In our no-choice experiments, we confined colonies to a single P:C substrate for 29 d (*M. smithii*), 39 d (*P. cornetzi*) or 15 d (*A. colombica*). We provide raw pre- and post-experiment colony demography data for colonies in Supplementary Table 5. For standardized comparison across these experiments with different attine species, intake data were analysed for 15 d across all colonies.

We calculated protein and carbohydrate use by the ants from the agar P:C ratios and substrate dry mass loss estimated from dry:wet mass ratios of control agar fragments for each P:C ratio[62]. We weighed colonies on the first (initial colony mass) and last day (final colony mass) of the experiments and calculated worker mortality rates by collecting all dead workers each time we changed substrates. During the *M. smithii* and *P. cornetzi* experiments, a number of colonies showed signs of crop failure (that is, elevated worker mortality or living workers ceasing foraging and discarding fungus garden material). For our demographic analyses, we assessed crops as having failed on the day colonies no longer had any fungus garden biomass left.

We performed statistical analyses in R version 3.2.4 (ref. [61]), exploring P:C substrate treatment effects on colony behaviour and performance separately for the three ant species (the *M. smithii* data were already similarly analysed in ref. [30]). We first used general linear models to test for substrate treatment effects on the response variables total macronutrient intake, protein intake and carbohydrate intake, with initial worker number as a covariate. These data were log-transformed before the analyses to meet the assumptions of normality and homoscedasticity. For both *A. colombica* and *P. cornetzi*, we analysed cumulative substrate use over 15 d. For *P. cornetzi*, we also analysed macronutrient use per day, with the number of days ranging from the full 39 d to any earlier day a specific colony was removed due to crop failure. Next, we performed a survival analysis (survfit, ggsurvplot) in R using a Cox proportional hazards model to test for substrate treatment effects on crop failure in *P. cornetzi*, including initial fungus garden mass as a covariate. This analysis was not used for *A. colombica* because no colonies exhibited crop failure. To further explore the links between foraging behaviour and colony demography in both *P. cornetzi* and *A. colombica*, we used general linear models to test for effects of P:C macronutrient mixes on changes in worker number and colony mass, analysing the slopes of linear regressions for each colony from values on day 1 to values on the final day of the experiment (day 39 in *P. cornetzi* and day 15 in *A. colombica*) or on the day the colony was removed from the experiment due to crop failure (a subset of *P. cornetzi* colonies).

RNNs of fungal cultivars estimated from field-collected substrates. To quantify RNNs for *P. cornetzi* and *M. smithii*, we first focused on cataloguing substrates harvested per unit time (Supplementary Table 7) and then on sampling the specific substrate categories to obtain sufficient biomass for nutritional analyses (Supplementary Table 9). We collected substrate items carried by laden workers returning to nests of 44 mapped *P. cornetzi* colonies from 08:00 to 16:00 during observation periods of ~1 h (43.7 total hours) (Supplementary Table 7). We collected substrates from 22 colonies of *M. smithii* using the same protocols, with sampling observations spanning over 20 h (Supplementary Table 7; see also ref. [30]). Some of the raw biomass data of collected substrates for *M. smithii* and *P. cornetzi* were previously published[40] but were here explicitly analysed as RNNs and compared with fungal FNNs (Fig. 4a). These collections occurred during the wet season (a period of high attine activity) from 16 November to 31 December in 2013 and 2 January to 17 January in 2014 (Supplementary Table 7). During observation periods, we lay on trash bags next to nest entrances, using a headlamp to maximize visibility, and carefully grabbed laden foragers with forceps just before they disappeared underground. We collected these substrate pieces in Eppendorf tubes and then dried them at 60 °C for 24 h before classifying them into six categories (insect frass, leaf fragment, wood, flower, seed or other (miscellaneous plant, insect piece or unknown)) and weighing them to the nearest 1 µg on a Sartorius CP2P microbalance. We then calculated the fraction of biomass of each substrate type relative to the total biomass of substrate collected.

For nutritional analyses, we first homogenized individual frass samples collected from 33 colonies of *P. cornetzi* and 19 colonies of *M. smithii* located

in the same leaf litter habitats as described above (Supplementary Table 9). We then determined their elemental carbon (percentage carbon) and nitrogen (percentage nitrogen) in the laboratory of B. Turner (STRI, Panama) with a Flash EA1112 analyser (CE Elantech). The small size of these substrate fragments precluded direct macronutrient-level analyses of their percentage of protein and carbohydrates. To acquire these macronutrient estimates, we used 30 1 m^2 tarps placed on leaf litter for 24-h intervals in the same forest in June 2019 to collect a large pooled sample of frass (and other detrital substrates) that fell from the canopy. Back in Copenhagen, we created a 1-g pooled frass sample of each substrate type (previously freeze-dried just after collection in Panama using an SP Scientific BenchTop Pro with Omnitronics for 24 h). We then homogenized these and analysed them for percentage carbon (using a Eurovector CN analyser coupled to an isoprime isotope ratio mass spectrometer in the laboratory of A. Michelsen at the University of Copenhagen), as well as the percentage of total non-structural carbohydrates (TNCs; water-soluble carbohydrates + starch). For the percentage of TNC measurements, we analysed 25 mg frass with a Total Carbohydrate Assay Kit (Sigma–Aldrich) to determine water-soluble carbohydrates, and 50 mg of frass with a Total Starch Assay Kit (Megazyme)[63] to quantify starch. We used five subsampled replicates for each quantification to calculate a conversion factor (2.59%) to substitute percentage carbon with percentage TNC for the frass and tiny wood fragments in the existing dataset (Supplementary Table 9).

From the elemental nitrogen frass data, we estimated crude protein (that is, including non-available protein bound up by tannins) by multiplying substrate nitrogen mass by the standard conversion factor 6.25, following the protocol reported by Felton et al.[63]. We then analysed percentage TNC in leaf litter samples of seeds ($n = 5$) and a flower ($n = 1$), as well as pooled samples of flowers ($n = 5$) and tiny wood bits ($n = 1$) (Supplementary Table 9). In these non-frass samples, we also quantified proteins using a CBQCA Protein Quantification Kit (Molecular Probes) (Supplementary Table 9).

The much larger quantities of fresh vegetative substrates harvested by leafcutter ants required different field collection methods and also facilitated more detailed near-infrared reflectance spectroscopy nutritional analyses that were not possible for the small amounts of tiny substrate particles harvested from the mandibles of palaeoattine and higher-neoattine (non-leafcutter) ants. In May 2019, we located an *A. colombica* colony at La Laguna (9.11672° W, −79.69514° N) and laid down on trash bags next to the most active trail, close to the nest entrance. We hand collected a total of 6,868 fragments (40,026 mg dry mass) carried by laden foragers during three 1.5-h periods by two observers (nine total collection hours) between 09:00 and 12:00 (Supplementary Table 8). These fragments (almost all fresh plant material) were stored in new Ziploc bags every 30 min that were promptly transferred to a cooler. Back in the laboratory, we catalogued the forage fragment samples under a microscope based on the morphology of the veins of leaf fragments, weighed the specific fractions and freeze-dried them for 24 h as described above.

We then stored the samples at −20 °C in new Ziploc bags with silica gel until subsequent nutrient and barcoding analyses. We extracted DNA from these samples and identified them using the internal transcribed spacer 1 (ITS1) genetic marker (details in Supplementary Methods; National Center for Biotechnology Information's GenBank accession codes provided in Supplementary Table 8). We then homogenized a subset of dried plant substrates into powder and used near-infrared reflectance spectroscopy[63] to estimate the concentrations of total nitrogen, total protein, TNCs and starch in all 17 plant substrates sampled (details provided in Supplementary Methods and Supplementary Table 12). The pie charts of harvested forage categories reported in Fig. 4 represent relative contributions to the total dry mass of substrate items collected by foraging workers (Supplementary Tables 7 and 8). Based on barcoding analyses, we pooled a subset of the 17 samples that were identified as coming from the same plant species, which gave a total of 13 plant species in the dataset (Supplementary Table 8). We converted the in vitro landscapes used to estimate cultivar FNNs from g l^{-1} to percentage protein and carbohydrates based on P:C diet recipes to directly compare these data with RNNs based on macronutrient content in the natural forage obtained in the field. For simplicity, only the extreme carbohydrate-biased (1:9 P:C) and protein-based (9:1 P:C) nutritional rails are plotted in Fig. 4 to delineate the range of in vitro P:C conditions under which cultivar FNNs were measured.

Obtaining accurate estimates of species diversity of sympatric farming systems. The single species status of *A. colombica* and its fungal cultivar *L. gongylophorus* in central Panama is not in question and the same applies for *M. smithii* except that this palaeoattine ant is known to be associated with a series of fungal cultivars[64], some of which were also recognized in our previous study of the nutritional geometry of this species[30]. However, this is much more ambiguous for *P. cornetzi* and its fungal symbionts, because a previous small-scale study[48] showed that there is substantial cryptic diversity not only among the cultivars but possibly also among the ants[48]. To avoid misinterpretations of our present results due to overlooking (and unjustifiably pooling) cryptic species of ants and cultivars, we performed an extensive survey across a large meta-population of *P. cornetzi* (54 km^2 of Soberanía Park forest) and within the local populations represented by our six 20 m^2 plots (Extended Data Fig. 10). Within these study plots, we mapped all higher-neoattine nests (*Paratrachymyrmex*, *Mycetomoellerius* and *Sericomyrmex*) by dispersing oat polenta bait in the leaf litter and following laden workers back to their nests ($n = 263$ total higher-neoattine nests across all plots; $n = 27 \pm 3$ searching hours per plot), and then collected two to four workers from each nest in vials with 95% ethanol. We also sampled workers from 85 additional *Paratrachymyrmex* and *Mycetomoellerius* colonies distributed across Soberanía Park, yielding 297 colonies sampled across these two genera. We similarly sampled 30 *A. colombica* colonies distributed across the Gamboa area.

We then identified the ants using morphological analysis of vouchers, as well as analysis of DNA microsatellite markers and mitochondrial DNA barcoding (details for each of these analyses are provided in the Supplementary Methods). Briefly, we used DNA microsatellite analyses to examine the population structure of workers from 28 *A. colombica* colonies (Extended Data Fig. 6) and 297 *Paratrachymyrmex* and *Mycetomoellerius* colonies (Extended Data Fig. 7) using a total of nine variable markers (Ant7680, Ant859, Ant1343, Ant2341, Ant3993, Ant11400, Ant3653, Ant4155 and Ant8498)[65]. To supplement these nuclear microsatellite data, we also used DNA barcoding analyses of a mitochondrial marker (~1,100 base pairs (bp) of the cytochrome *c* oxidase 1 gene), which included ant workers from 147 *Paratrachymyrmex*, 38 *Mycetomoellerius* and 29 *A. colombica* colonies (Supplementary Table 13). A subset of these ants were paired with their fungal cultivars to examine farmer–cultivar association patterns, as we excavated 69 colonies of putative *P. cornetzi* and 29 colonies of *A. colombica* (Supplementary Table 14). For each of these colonies, we collected a clean 2 cm^3 fraction of fungus garden with forceps into vials with 95% ethanol soon after excavation. We identified these samples by analysing mitochondrial DNA (~820 bp of the nuclear large subunit (LSU) ribosomal RNA and ~550 bp of the ITS). We used these sequences (plus sequences from an additional *M. smithii* ant and fungal sample) to generate phylogenetic trees (details about tree generation are provided in the Supplementary Methods).

The resulting sequence information and supporting dataset for the 215 ant specimens is named DS-ATTINENG "Nutritional niches reveal fundamental domestication trade-offs in fungus-farming ants" and has been deposited in the Barcode of Life Data System[66] (BOLD; http://dx.doi.org/10.5883/DS-ATTINENG). The sequence data are also deposited in GenBank (with accession codes provided in Supplementary Table 13). The sequence information for 99 fungal cultivar samples in Fig. 5 has been deposited in GenBank (accession codes for LSU and ITS are provided in Supplementary Table 14). To further interpret our molecular evidence confirming known species and detecting cryptic species among the collected *P. cornetzi*-like colonies within Soberanía Park, we also explored the biogeographic distribution of this species complex by comparing our sequence data with the sequences of eight Costa Rican and one Ecuadorian *P. cornetzi* ant specimens available from BOLD[66] (Extended Data Fig. 8).

Cultivar diversity across colonies, in vitro FNN variation and growth performance. We visualized the FNNs of isolated cultivars (Fig. 6a) from three colonies of *P. cornetzi* (177605, 177611 and 177612) and three colonies of *A. colombica* (177627, 177628 and 177626) (Supplementary Table 3). Cultivars were selected before determining their haplotype identity, after which the *P. cornetzi* cultivars used in the experiment were identified as haplotype 1 (177605 and 177612) and haplotype 3 (177612) (Fig. 6a). Due to general differences in growth rate among cultivar haplotypes on standard PDA medium, these haplotypes were grown on P:C substrates for different lengths of time (Supplementary Table 3). A trained researcher (M.F.) also estimated the staphyla production rate (staphyla number per number of growth days) by visually scanning the high-resolution photos and validating counts by opening a subset of plates and directly counting staphyla (clusters of gongylidia) under a dissecting microscope at 40× magnification.

Reporting Summary. Further information on research design is available in the Nature Research Reporting Summary linked to this article.

Data availability

The DNA sequences generated during this study are available from the National Center for Biotechnology Information's GenBank database. This includes the data for the 215 ant specimens (accession codes for the cytochrome *c* oxidase I sequences are provided in Supplementary Table 13), the 99 fungal cultivar samples (accession codes for the LSU and ITS sequences are provided in Supplementary Table 14) and plant sample ITS1 sequences harvested by colonies of *A. colombica* (accession codes are provided in Supplementary Table 8). Ant sequence datasets and supporting information are also deposited in BOLD[66] under the project titled DS-ATTINENG "Nutritional niches reveal fundamental domestication trade-offs in fungus-farming ants" (http://dx.doi.org/10.5883/DS-ATTINENG).

Code availability

No custom code was generated for this study. The sequence alignment matrices and Newick files used to generate the phylogenies shown in Fig. 5 (both fungal and ant trees) and Extended Data Fig. 8 are available as text files in Supplementary Data 1–3. All of the code used to generate the results will be made available upon request.

Received: 9 February 2020; Accepted: 25 August 2020;
Published online: 26 October 2020

References

1. Piperno, D. & Pearsall, D. M. *The Origins of Agriculture in the Lowland Neotropics* (Academic Press, 1998).
2. Newell-McGloughlin, M. Nutritionally improved agricultural crops. *Plant Physiol.* **147**, 939–953 (2008).
3. Green, R. E., Cornell, S. J., Scharlemann, J. P. W. & Balmford, A. Farming and the fate of wild nature. *Science* **307**, 550–555 (2005).
4. Meyer, R. S., DuVal, A. E. & Jensen, H. R. Patterns and processes in crop domestication: an historical review and quantitative analysis of 203 global food crops. *New Phytol.* **196**, 29–48 (2012).
5. Purugganan, M. D. & Fuller, D. Q. The nature of selection during plant domestication. *Nature* **457**, 843–848 (2009).
6. Milla, R., Osborne, C. P., Turcotte, M. M. & Violle, C. Plant domestication through an ecological lens. *Trends Ecol. Evol.* **30**, 463–469 (2015).
7. Evans L. T. *Crop Evolution, Adaptation and Yield* (Cambridge Univ. Press, 1993)
8. Turcotte, M. M., Turley, N. E. & Johnson, M. T. J. The impact of domestication on resistance to two generalist herbivores across 29 independent domestication events. *New Phytol.* **204**, 671–681 (2014).
9. Chomicki, G. & Renner, S. S. Farming by ants remodels nutrient uptake in epiphytes. *New Phytol.* **223**, 2011–2023 (2019).
10. Mueller, U. G., Gerardo, N. M., Aanen, D. K., Six, D. L. & Schultz, T. R. The evolution of agriculture in insects. *Annu. Rev. Ecol. Evol. Systemat.* **36**, 563–595 (2005).
11. Aanen, D. K. et al. The evolution of fungus-growing termites and their mutualistic fungal symbionts. *Proc. Natl Acad. Sci. USA* **99**, 14887–14892 (2002).
12. Mehdiabadi, N. J. & Schultz, T. R. Natural history and phylogeny of the fungus-farming ants (Hymenoptera: Formicidae: Myrmicinae: Attini). *Myrmecol. News* **13**, 37–55 (2009).
13. Mueller, U. G., Scott, J. J., Ishak, H. D., Cooper, M. & Rodrigues, A. Monoculture of leafcutter ant gardens. *PLoS ONE* **9**, e12668 (2010).
14. Schultz, T. R. & Brady, S. G. Major evolutionary transitions in ant agriculture. *Proc. Natl Acad. Sci. USA* **105**, 5435–5440 (2008).
15. Kooij, P. W., Aanen, D. K., Schiøtt, M. & Boomsma, J. J. Evolutionary advanced ant farmers rear polyploid fungal crops. *J. Evol. Biol.* **28**, 1911–1924 (2015).
16. Shik, J. Z. et al. Metabolism and the rise of fungus cultivation by ants. *Am. Nat.* **184**, 364–373 (2014).
17. De Fine Licht, H. H. et al. Laccase detoxification mediates the nutritional alliance between leaf-cutting ants and fungus-garden symbionts. *Proc. Natl Acad. Sci. USA* **110**, 583–587 (2012).
18. Fernández-Marín, H. et al. Functional role of phenylacetic acid from metapleural gland secretions in controlling fungal pathogens in evolutionarily derived leaf-cutting ants. *Proc. R. Soc. B* **282**, 20150212 (2015).
19. Fernández-Marín, H. et al. Dynamic disease management in *Trachymyrmex* fungus-growing ants (Attini: Formicidae). *Am. Nat.* **181**, 571–582 (2013).
20. Currie, C. R., Mueller, U. G. & Malloch, D. The agricultural pathology of ant fungus gardens. *Proc. Natl Acad. Sci. USA* **96**, 7998–8002 (1999).
21. Nygaard, S. et al. Reciprocal genomic evolution in the ant–fungus agricultural symbiosis. *Nat. Commun.* **7**, 12233 (2016).
22. Branstetter, M. G. et al. Dry habitats were crucibles of domestication in the evolution of agriculture in ants. *Proc. R. Soc. B* **284**, 20170095 (2017).
23. Li, H. et al. Convergent evolution of complex structures for ant–bacterial defensive symbiosis in fungus-farming ants. *Proc. Natl Acad. Sci. USA* **115**, 10720–10725 (2018).
24. Hölldobler, B. & Wilson, E. O. *The Leafcutter Ants: Civilization by Instinct* (W. W. Norton & Company, 2010).
25. Mueller, U. G. et al. Evolution of cold-tolerant fungal symbionts permits winter fungiculture by leafcutter ants at the northern frontier of a tropical ant–fungus symbiosis. *Proc. Natl Acad. Sci. USA* **108**, 4053–4056 (2011).
26. Simpson, S. J. & Raubenheimer, D. *The Nature of Nutrition: A Unifying Framework from Animal Adaptation to Human Obesity* (Princeton Univ. Press, 2012).
27. Raubenheimer, D. Toward a quantitative nutritional ecology: the right-angled mixture triangle. *Ecol. Monogr.* **81**, 407–427 (2011).
28. Sperfeld, E. et al. Bridging ecological stoichiometry and nutritional geometry with homeostasis concepts and integrative models of organism nutrition. *Funct. Ecol.* **31**, 286–296 (2017).
29. Shik, J. Z. & Dussutour, A. Nutritional dimensions of invasive success. *Trends Ecol. Evol.* **35**, 691–703 (2020).
30. Shik, J. Z. et al. Nutrition mediates the expression of cultivar–farmer conflict in a fungus-growing ant. *Proc. Natl Acad. Sci. USA* **113**, 10121–10126 (2016).
31. Machovsky-Capuska, G. E., Senior, A. M., Simpson, S. J. & Raubenheimer, D. The multidimensional nutritional niche. *Trends Ecol. Evol.* **31**, 355–365 (2016).
32. Masiulionis, V. E. et al. A Brazilian population of the asexual fungus-growing ant *Mycocepurus smithii* (Formicidae, Myrmicinae, Attini) cultivates fungal symbionts with gongylidia-like structures. *PLoS ONE* **9**, e103800 (2014).
33. Vo, T. L., Mikheyev, A. S. & Mueller, U. G. Free-living fungal symbionts (Lepiotaceae) of fungus-growing ants (Attini: Formicidae). *Mycologia* **101**, 206–210 (2009).
34. Schultz, T. R. et al. The most relictual fungus-farming ant species cultivates the most recently evolved and highly domesticated fungal symbiont species. *Am. Nat.* **185**, 693–703 (2015).
35. Solomon, S. E. et al. The molecular phylogenetics of *Trachymyrmex* Forel ants and their fungal cultivars provide insights into the origin and coevolutionary history of 'higher-attine' ant agriculture. *Syst. Entomol.* **44**, 939–956 (2019).
36. Quinlan, R. J. & Cherrett, J. M. The role of fungus in the diet of the leaf-cutting ant *Atta cephalotes* (L.). *Ecol. Entomol.* **4**, 151–160 (1979).
37. Schiøtt, M., de Fin Licht, H. H., Lange, L. & Boomsma, J. J. Towards a molecular understanding of symbiont function: identification of a fungal gene for the degradation of xylan in the fungus gardens of leaf cutting ants. *BMC Biol.* **8**, 40 (2008).
38. De Fine Licht, H. H., Boomsma, J. J. & Tunlid, A. Symbiotic adaptations in the fungal cultivar of leaf-cutting ants. *Nat. Commun.* **5**, 5675 (2014).
39. De Fine Licht, H. H. & Boomsma, J. J. Forage collection, substrate preparation, and diet composition in fungus-growing ants. *Ecol. Ent.* **35**, 259–269 (2010).
40. Sapountzis, P., Zhukova, M., Shik, J. Z., Schiøtt, M. & Boomsma, J. J. Reconstructing the symbiotic functions of intestinal Mollicutes in fungus-growing ants. *eLife* **7**, e39209 (2018).
41. Seal, J. N. & Tschinkel, W. R. Colony productivity of the fungus-gardening ant *Trachymyrmex septentrionalis* (Hymenoptera: Formicidae) in a Florida pine forest. *Ann. Ent. Soc. Am.* **99**, 673–682 (2006).
42. Wirth, R., Beyschlag, W., Ryel, R. J. & Hölldobler, B. Annual foraging of the leaf-cutting ant *Atta colombica* in a semideciduous rain forest in Panama. *J. Trop. Ecol.* **13**, 741–757 (1997).
43. Cazin, J. Jr., Wiemer, D. F. & Howard, J. J. Isolation, growth characteristics, and long-term storage of fungi cultivated by attine ants. *Appl. Environ. Microbiol.* **55**, 1346–1350 (1989).
44. Mueller, U. G., Schultz, T. R., Currie, C. R., Adams, R. M. M. & Malloch, D. The origin of the attine ant–fungus mutualism. *Quart. Rev. Biol.* **76**, 169–197 (2001).
45. De Fine Licht, H. H., Schiøtt, M., Mueller, U. G. & Boomsma, J. J. Evolutionary transitions in enzyme activity of ant fungus gardens. *Evolution* **64**, 2055–2069 (2010).
46. Chapela, I. H., Rehner, S. A., Schultz, T. R. & Mueller, U. G. Evolutionary history of the symbiosis between fungus-growing ants and their fungi. *Science* **266**, 1691–1694 (1994).
47. Mikheyev, A. S., Mueller, U. G. & Boomsma, J. J. Population genetic signatures of diffuse co-evolution between leaf-cutting ants and their cultivar fungi. *Mol. Ecol.* **16**, 209–216 (2007).
48. De Fine Licht, H. H. & Boomsma, J. J. Variable interaction specificity and symbiont performance in Panamanian *Trachymyrmex* and *Sericomyrmex* fungus-growing ants. *BMC Evol. Biol.* **14**, 244 (2014).
49. Howe, J., Schiøtt, M. & Boomsma, J. J. Horizontal partner exchange does not preclude stable mutualism in fungus-growing ants. *Behav. Ecol.* **30**, 372–382 (2018).
50. Cornejo, F. H., Varela, A. & Wright, S. J. Tropical forest litter decomposition under seasonal drought: nutrient release, fungi and bacteria. *Oikos* **70**, 183–190 (1994).
51. Wilson, E. O. Caste and division of labor in leaf-cutter ants (Hymenoptera: Formicidae: *Atta*). II. The ergonomic optimization of leaf cutting. *Behav. Ecol. Sociobiol.* **7**, 157–165 (1980).
52. Roces, F. & Hölldobler, B. Use of stridulation in foraging leaf-cutting ants: mechanical support during cutting or short-range recruitment signal? *Behav. Ecol. Sociobiol.* **39**, 293–299 (1996).
53. Kleineidam, C., Romani, R., Tautz, J. & Isidoro, N. Ultrastructure and physiology of the CO_2 sensitive sensillum ampullaceum in the leaf-cutting ant *Atta sexdens*. *Arthropod Struct. Dev.* **29**, 43–55 (2000).
54. Sapountzis, P., Nash, D. R., Schiøtt, M. & Boomsma, J. J. The evolution of abdominal microbiomes in fungus-growing ants. *Mol. Ecol.* **28**, 879–899 (2019).
55. Pinto-Tomás, A. A. et al. Symbiotic nitrogen fixation in the fungus gardens of leaf-cutter ants. *Science* **326**, 1120–1123 (2009).
56. Mummert, A. E., Esche, E., Robinson, J. & Armelagos, G. J. Stature and robusticity during the agricultural transition: evidence from the bioarchaeological record. *Econ. Hum. Biol.* **9**, 284–301 (2011).
57. Fuller, D. Q. et al. The domestication process and domestication rate in rice: spikelet bases from the Lower Yangtze. *Science* **323**, 1607–1610 (2009).
58. Sauer, C. O. *Agricultural Origins and Dispersals* (American Geographical Society, 1952).

59. Nuotclà, J. A., Biedermann, P. H. W. & Taborsky, M. Pathogen defence is a potential driver of social evolution in ambrosia beetles. *Proc. R. Soc. B* **286**, 20192332 (2019).
60. Nychka, D., Furrer, R. & Sain, S. Fields: Tools for spatial data. R package version 8.2-1 https://cran.r-project.org/web/packages/fields/index.html (2015).
61. R Core Development Team *R: A Language and Environment for Statistical Computing* (R Foundation for Statistical Computing, 2018).
62. Kay, A. D., Shik, J. Z., Van Alst, A., Miller, K. A. & Kaspari, M. Diet composition does not affect ant colony tempo. *Funct. Ecol.* **26**, 317–323 (2011).
63. Felton, A. M. et al. Nutritional ecology of *Ateles chamek* in lowland Bolivia: how macronutrient balancing influences food choices. *Int. J. Primatol.* **30**, 675–696 (2009).
64. Kellner, K., Fernández-Marín, H., Ishak, H. D., Linksvayer, T. A. & Mueller, U. G. Co-evolutionary patterns and diversification of ant–fungus associations in the asexual fungus-farming ant *Mycocepurus smithii* in Panama. *J. Evol. Biol.* **26**, 1353–1362 (2013).
65. Butler, I. A., Siletti, K., Oxley, P. R. & Kronauer, D. J. C. Conserved microsatellites in ants enable population genetic and colony pedigree studies across a wide range of species. *PLoS ONE* **9**, e107334 (2014).
66. Ratnasingham, S. & Hebert, P. D. N. BOLD: the Barcode of Life Data System (www.barcodinglife.org). *Mol. Ecol. Notes* **7**, 355–364 (2007).
67. Dussutour, A., Latty, T., Beekman, M. & Simpson, S. J. Amoeboid organism solves complex nutritional challenges. *Proc. Natl Acad. Sci. USA* **107**, 4607–4611 (2010).
68. Dussutour, A. & Simpson, S. J. Description of a simple synthetic diet for studying nutritional responses in ants. *Insect. Soc.* **55**, 329–333 (2008).
69. Dussutour, A. & Simpson, S. J. Communal nutrition in ants. *Curr. Biol.* **19**, 740–744 (2009).
70. Warbrick-Smith, J., Raubenheimer, D., Simpson, S. J. & Behmer, S. T. Three hundred and fifty generations of extreme food specialisation: testing predictions of nutritional ecology. *Entomol. Exp. Appl.* **132**, 65–75 (2009).

Acknowledgements

STRI provided support and access to facilities in Gamboa. The Autoridad Nacional del Ambiente y el Mar (ANAM) gave permission to the laboratory groups of J.J.B. and J.Z.S. to sample attine ants in Panama and export them to Denmark. We thank students of the Tropical Behavioural Ecology and Evolution field course in 2015 for additional assistance with collecting colonies. J.Z.S. was supported by a postdoctoral fellowship via a Smithsonian Institution Competitive Grant to W.T.W., J.J.B. and J.Z.S., an EU Marie Sklodowska-Curie International Incoming Fellowship (327940), the Centre for Social Evolution at the University of Copenhagen (Danish National Research Foundation: DNRF57), an ERC Advanced grant (ANTS: 323085) to J.J.B. and an ERC Starting Grant to J.Z.S. (ELEVATE: 757810). J.C.S. was supported by SJU start-up funds and NSF-DEB number 2016372.

Author contributions

J.Z.S., J.J.B. and W.T.W. conceived of and designed the study. J.Z.S., E.B.G., M.F., A.J.J.C., D.A.D. and P.W.K. performed the fieldwork, collected the colonies, isolated the fungal cultivars and performed the in vitro experiments with fungal cultivars. D.A.D., J.Z.S., P.W.K. and A.J.J.C. extracted DNA and performed DNA barcoding analyses for ants and fungal cultivars. P.W.K., J.Z.S. and J.H. performed the microsatellite analyses. X.A. and J.Z.S. performed the statistical analyses. J.C.S. performed the phylogenetics analyses. J.Z.S. and J.J.B. wrote the initial draft of the manuscript. J.Z.S., P.W.K., D.A.D., J.C.S., A.J.J.C., X.A., J.H., W.T.W. and J.J.B. contributed to interpreting the data and editing subsequent drafts of the manuscript.

Competing interests

The authors declare no competing interests.

Additional information

Extended data is available for this paper at https://doi.org/10.1038/s41559-020-01314-x.

Supplementary information is available for this paper at https://doi.org/10.1038/s41559-020-01314-x.

Correspondence and requests for materials should be addressed to J.Z.S.

Reprints and permissions information is available at www.nature.com/reprints.

Publisher's note Springer Nature remains neutral with regard to jurisdictional claims in published maps and institutional affiliations.

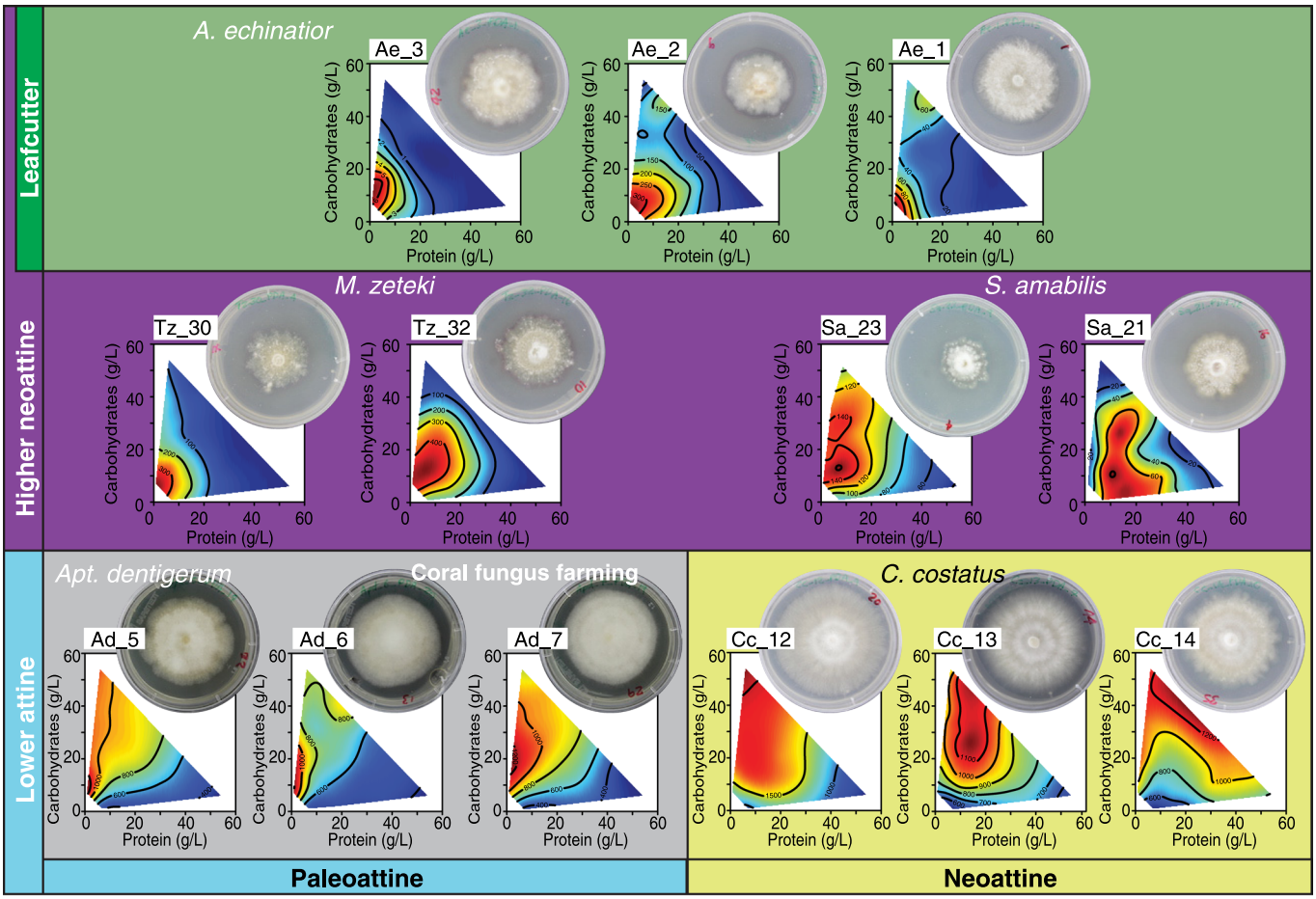

Extended Data Fig. 1 | Cultivars exhibited consistent FNNs for hyphal growth when isolated from different colonies of each attine species, supporting that the heatmaps based on species means (Fig. 2, Fig. 4b,c) accurately represent each cultivar's FNN. Additional details about how these heatmaps were generated and how they were interpreted are provided in Fig. 2. Heatmaps are provided here for attine species where multiple colonies were sampled. Additional colony-level heatmaps for *P. cornetzi* and *A. colombica* are provided in Fig. 6a. Collection IDs corresponding to experiment IDs were: Ae_3 [177625], Ae_2 [177624], Ae_1 [177609], Tz_30 [177632], Tz_32 [177634], Sa_23 [177623], Sa_21 [177614], Ad_5 [177629], Ad_6 [177630], Ad_7 [177631], Cc_12 [37861], Cc_13 [37862], and Cc14 [37864] (Supplementary Table 3). As in Fig. 2, least-square regressions showed that each of the response surface regressions producing the heatmap colour-gradients was significant (Supplementary Table 1).

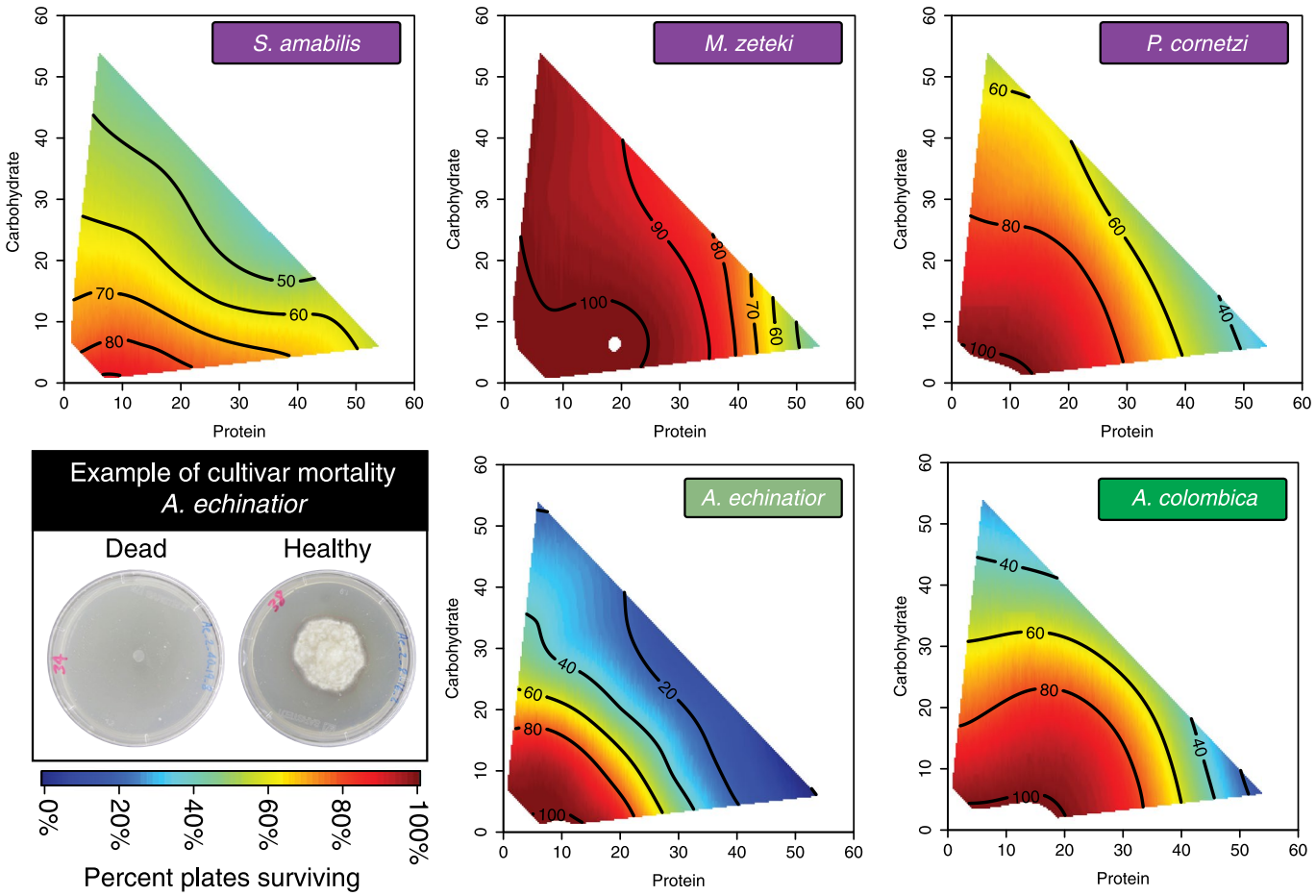

Extended Data Fig. 2 | Cultivars of the higher-neoattine genera *Sericomyrmex*, *Mycetomoellerius*, *Paratrachymyrmex* (purple) and the leafcutter genera *Acromyrmex* (light green) and *Atta* (dark green) often exhibited mortality when confined to media with macronutrient mixtures outside their FNNs. As shown in the figure legend, dark red indicates 100% survival and dark blue indicates 0% survival (a clear inoculation plug or a failure to colonize the agar plate from the inoculation plug). Percent mortality data were averaged across cultivars isolated from colonies of the same attine species (n = 2, *M. zeteki*; n = 3, *P. cornetzi*; n = 1, *S. amabilis*; n = 3, *A. echinatior*; n = 3, *A. colombica*, Supplementary Table 2). Mortality data were not recorded for the *S. amabilis* colony Sa_23. Small white areas on some of the plots indicate 100% survival.

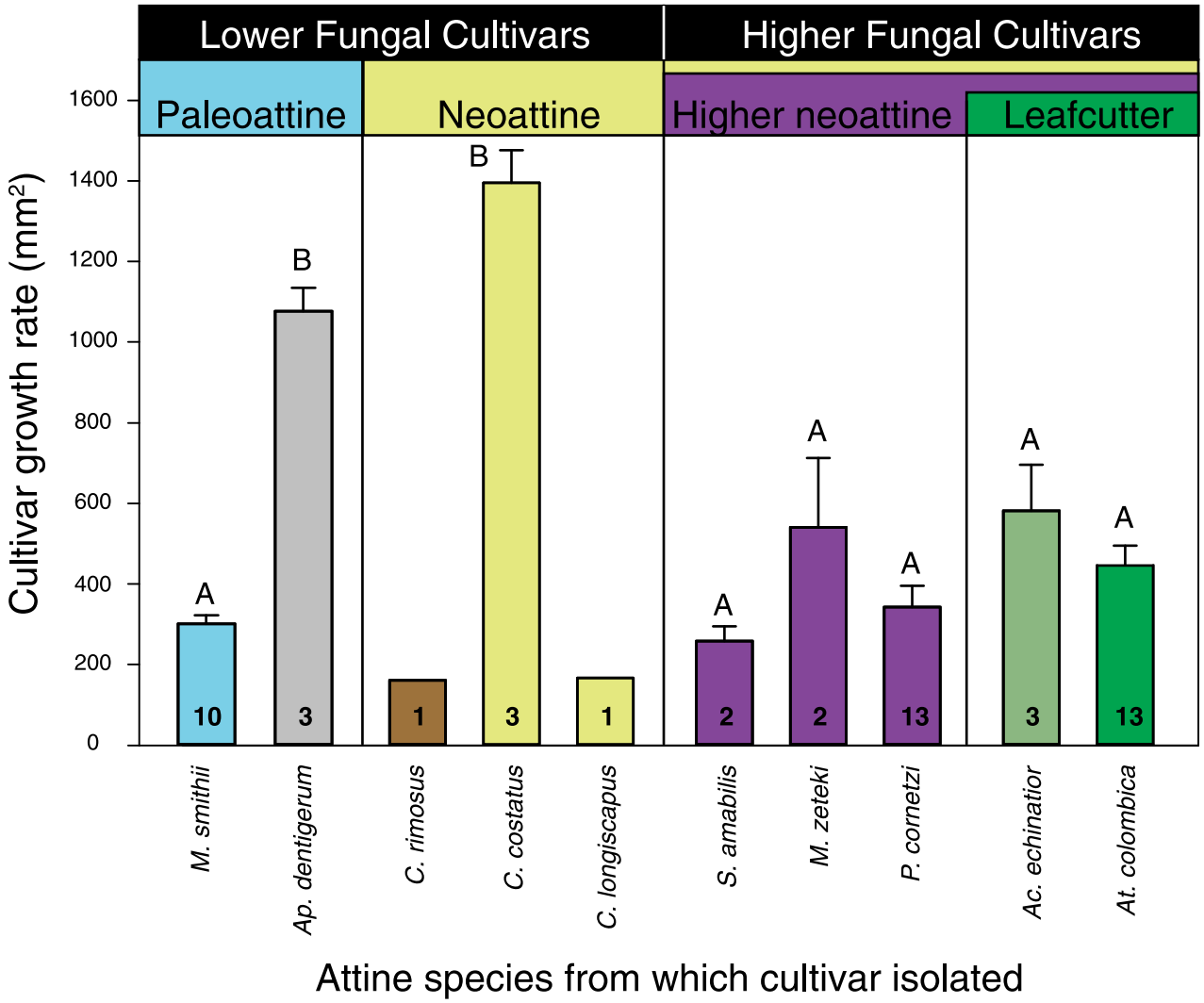

Extended Data Fig. 3 | The emergence of large-scale fungus farming by *Atta* leafcutter ants cannot be explained solely by an increase in intrinsic cultivar growth rate. Coloured bars (corresponding to the farming transitions in the schematic tree of Fig. 1a) represent *in vitro* growth rates of cultivars during 30 days on a standard PDA medium. Vertical lines separate the major farming transitions that distinguish ten attine species sympatrically inhabiting the Panamanian rainforest of Soberanía park (see caption Fig. 1a). ANOVA showed that attine species farmed cultivars with significantly different growth rates after 30-days ($F_{7,41} = 24.42$, $p < 0.0001$) and letters indicate pairwise differences that were significant at $P < 0.05$ in post-hoc Tukey tests. Numbers inside bars indicate numbers of colonies from which cultivars were isolated and used to calculate mean growth rates (+ SE) (Supplementary Table 3). The cultivars of *C. rimosus* and *C. longiscapus* were not included in the statistical analyses because we had no replicate colonies for these two ant species.

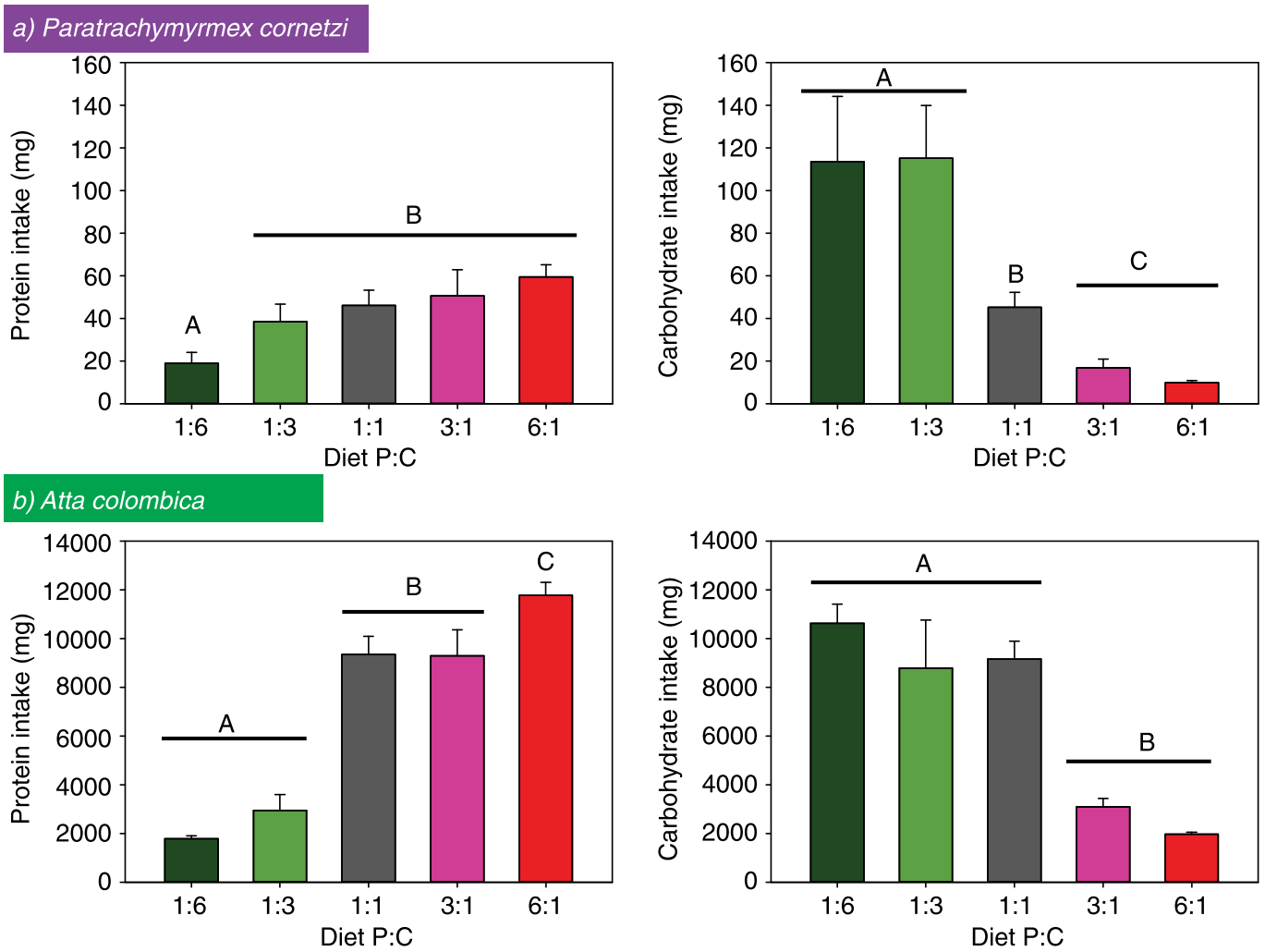

Extended Data Fig. 4 | Cumulative amounts of protein and carbohydrates collected over 15 days by whole colonies of a) *P. cornetzi* and b) *A. colombica*. While colonies of *P. cornetzi* and *M. smithii*[30] avoided protein-biased substrates with ratios above 1:3 P:C, colonies of *A. colombica* collected large amounts of the 1:1 P:C agar that *P. cornetzi* and *M. smithii* avoided. Colonies of *A. colombica* further collected statistically similar levels of carbohydrates on 1:1, 1:3, and 1:6 P:C substrates (Supplementary Table 4). This tolerance of higher protein levels enables *A. colombica* to sustain higher carbohydrate intake levels on 1:1 P:C diets. Letters indicate pairwise differences that were significant at $P < 0.05$ (post-hoc Tukey tests) (Supplementary Table 4). These intake plots (means + SE) provide an alternative single-nutrient presentation of the bi-variate intake data presented in Fig. 3b.

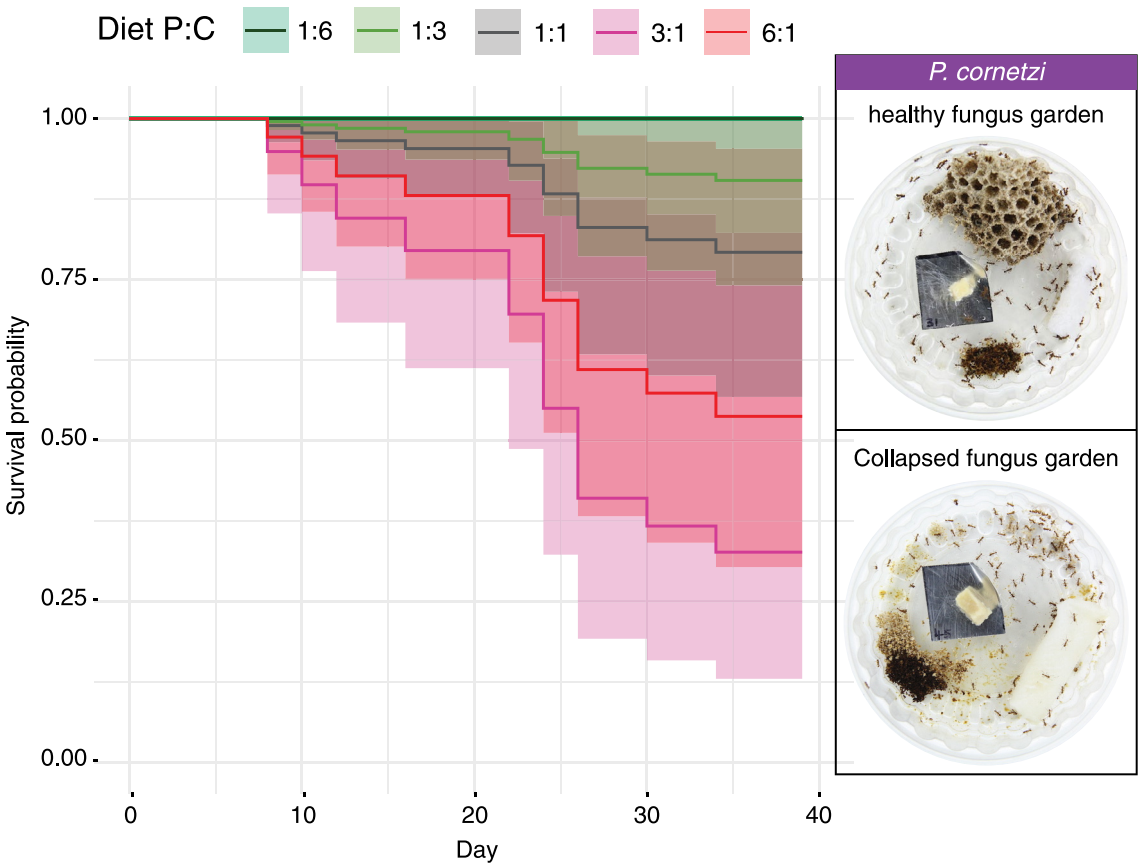

Extended Data Fig. 5 | Colonies of *P. cornetzi* increasingly faced crop failure when confined to P:C macronutrient mixtures with excess protein relative to carbohydrates ($\chi^2_4 = 17.9$; $p = 0.001$). While similar results were observed for *M. smithii*[30], no colonies of *A. colombica* experienced crop failure, even when confined to the same protein-biased substrates. Cultivar survival probabilities were estimated with a Cox proportional hazards model where substrate treatment was the explanatory variable, initial garden mass was a covariate, and days remaining in the feeding experiment was the response variable.

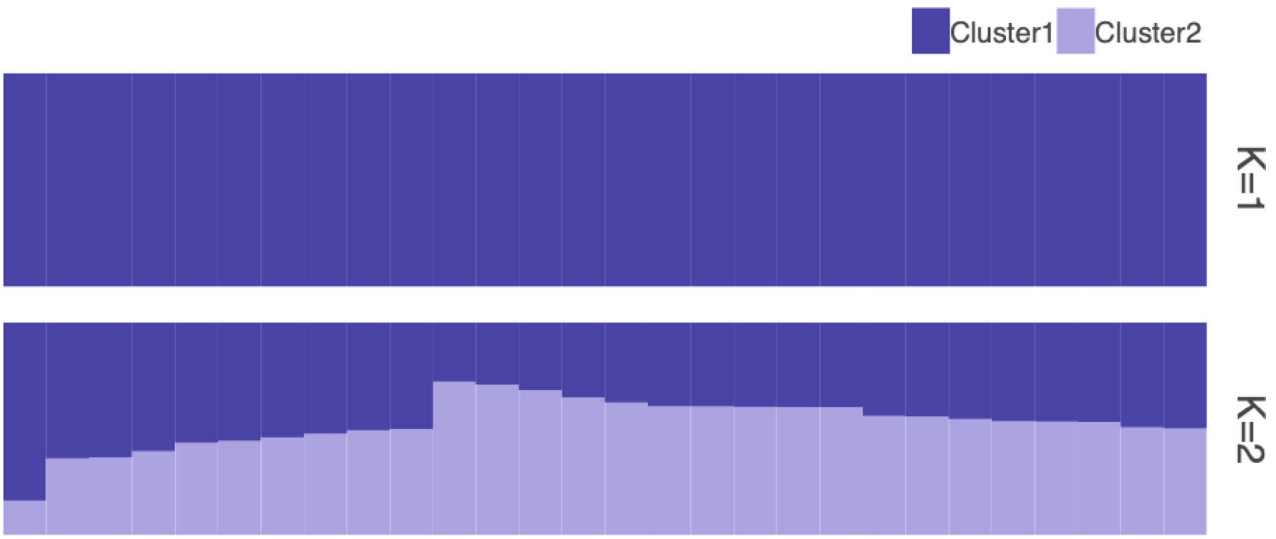

Extended Data Fig. 6 | STRUCTURE analyses of 9 microsatellite loci indicated that workers from 28 *Atta colombica* colonies in the Gamboa area of Soberanía park represent a single interbreeding population. Specifically, the mean log-likelihood was highest at $K=1$ (although ΔK cannot be assessed at $K=1$). When K was set to two, no individuals could be assigned to a single cluster. This Structure plot included a burn-in of 250,000, MCMC reps of 500,000 and 25 iterations per K.

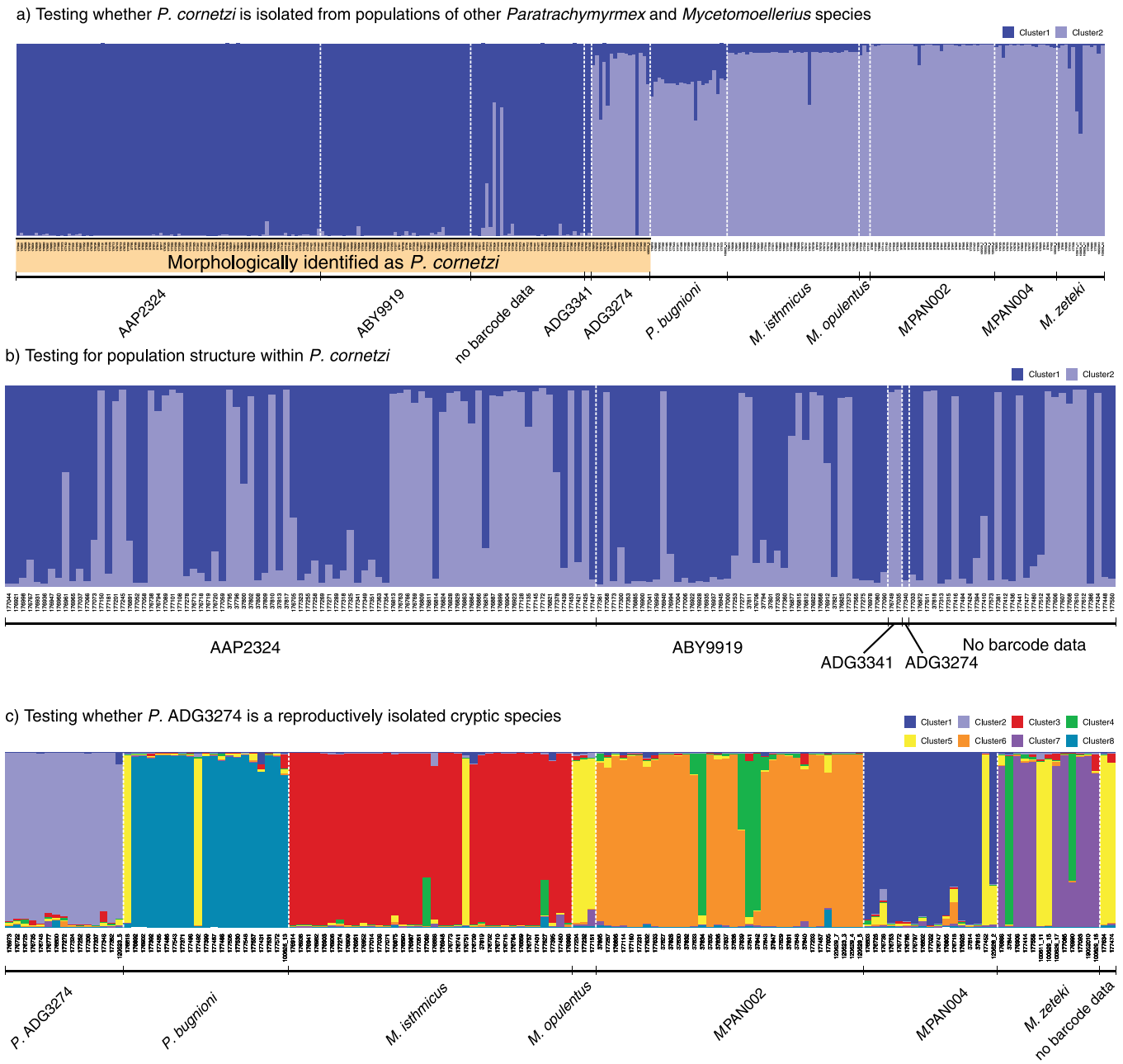

Extended Data Fig. 7 | See next page for caption.

Extended Data Fig. 7 | STRUCTURE analyses of nuclear genetic marker data from nine microsatellite loci from 297 *Paratrachymyrmex* and *Mycetomoellerius* workers, from 194 and 103 colonies respectively, indicate that *P. cornetzi* and *P.* ADG3274 represent distinct ant species within the total community of eight species belonging to these two ant genera in Soberanía Park. a, A STRUCTURE analysis across all samples (N = 297) indicated that the most likely population subdivision is two species because K = 2 reached the highest (ΔK) resolution (burn-in 200000, MCMC reps = 5000000, 25 iterations per K). This analysis separated samples that were all previously identified as *P. cornetzi* using morphological characters. It also grouped three Barcode of Life Data System[66] (www.boldsystems.org) haplotypes (AAP2324, ABY9919, ADG3341) separately from the newly recognized cryptic species *P.* ADG3274, that otherwise clustered with the remaining species (light blue). Although ΔK cannot be calculated for $K = 1$, the log-likelihood at $K = 1$ (−11121.864) was substantially lower than the one at $K = 2$ (−9397.616), suggesting that 'no population subdivision' is unlikely, consistent with all other species being morphologically distinct. **b,** A similar STRUCTURE analysis using those individuals assigned to cluster 1 in panel a (N = 156) indicated that three barcoded haplotypes (AAP2324, ABY9919, ADG3341) located in the BOLD database represent a single interbreeding population within Soberanía Park called *P. cornetzi*. Specifically, ΔK was highest at 2 (1305.79) but the mean log-likelihood was similar for K = 1 (−3849.092) and K = 2 (−3698.860), suggesting that any existing population structure here is weak. The haplotypes also do not separate the dark blue and light blue bars across our sampling sites consistent with failure to reliably assign individual workers to clusters 1 or 2 as expected under high admixture rates. One sample was identified as *P.* ADG3274 by barcoding analysis (177340) (Fig. 5, Extended Data Fig. 8), but could not be reliably distinguished from *P. cornetzi* by this STRUCTURE analysis. **c,** A STRUCTURE plot generated for the remaining (non-*P. cornetzi*) individuals (N = 156), indicated that $K = 8$ was the most likely subdivision, with little to no admixture between these species. The cryptic species *P.* ADG3274 forms a distinct cluster in this analysis. These genetic species assignments correspond well to species identities obtained by morphological criteria and barcoding (Extended Data Fig. 8) and included four currently named species (*P. bugnioni*, *M. isthmicus*, *M. opulentus*, and *M. zeteki*), and three unnamed species (*M.* PAN004 and *M.* PAN002, and *P.* ADG3274). The ants *M.* PAN004 and *M.* PAN002 were placed in the genus *Mycetomoellerius*[35] since they grouped with *M. isthmicus*, *M. opulentus*, and *M. zeteki* in the CO1 barcoding tree (Extended Data Fig. 8, Supplementary Table 13) and because they exhibited the required morphological characters to justify this decision. This STRUCTURE analysis also suggested there are potentially more than one species within the *M. zeteki* and *M.* PAN002 clusters, and that six stray samples (yellow bars) may also be distinct despite being morphologically grouped similar to *P. bugnioni* (n = 2 samples), *M. isthmicus* (n = 1), *T.* PAN004 (n = 1), and *M. zeteki* (n = 2). Overall, the results of this analysis confirm that perhaps only ~ half of the species are known even in a well-studied insect group in the tropics. The potential taxonomic implications of the *P. cornetzi* and *P.* ADG3274 species complex are beyond the scope of the present study. Samples labelled with "no barcode" were ants that were identified as belonging to *Paratrachymyrmex* and *Mycetomoellerius* using morphological characters but were not included in barcoding analyses.

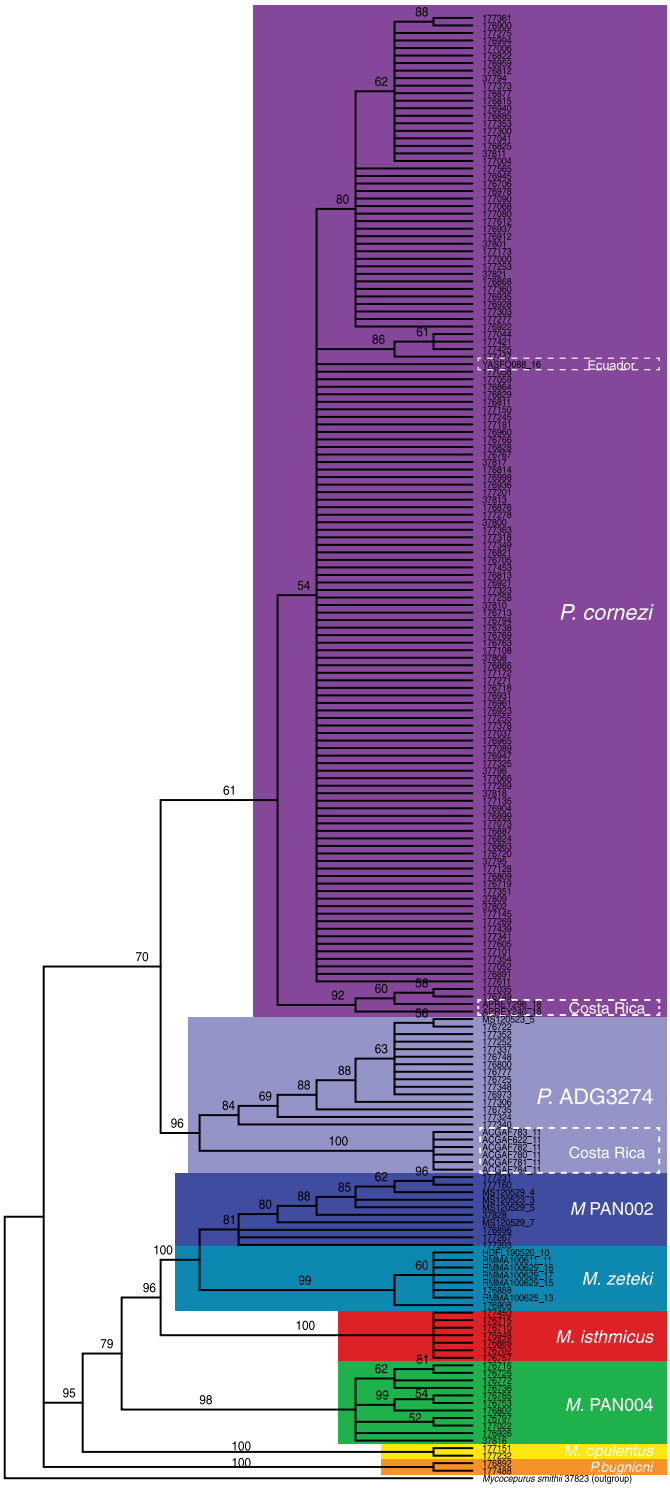

Extended Data Fig. 8 | A majority-rule consensus tree based on COI sequences of 185 *Paratrachymyrmex and Mycetomoellerius* ants supported our microsatellite analyses as the same eight species were recognized as co-occurring across Soberanía National Park. Three of these species belonged to the genus *Paratrachymyrmex* (*P. cornetzi* [n = 130], *P.* ADG3274 [n = 15], *P. bugnioni* [n = 2]) and five belonged to the genus *Mycetomoellerius* (*M. zeteki* [n = 8], *M. opulentus* [n = 2], *M. isthmicus* [n = 7], *M.* PAN002 [n = 10], *M.* PAN004 [n = 11]; Supplementary Table 13)[22,35] which is sister to the genus *Sericomyrmex*. This tree contains 9 additional public *P. cornetzi* COI sequences deposited at the Barcode of Life Data System database[66] (BOLD, www.boldsystems.org) that supported that the main *P. cornetzi* haplotype occurs at least from Ecuador to Costa Rica (N = 3 specimens), and that the cryptic *P. cornetzi* haplotype [ADG3274] is distributed at least from the Canal Zone in Panama to La Selva forest in Costa Rica (N = 6 specimens). The tree was rooted by a worker of *M. smithii*.

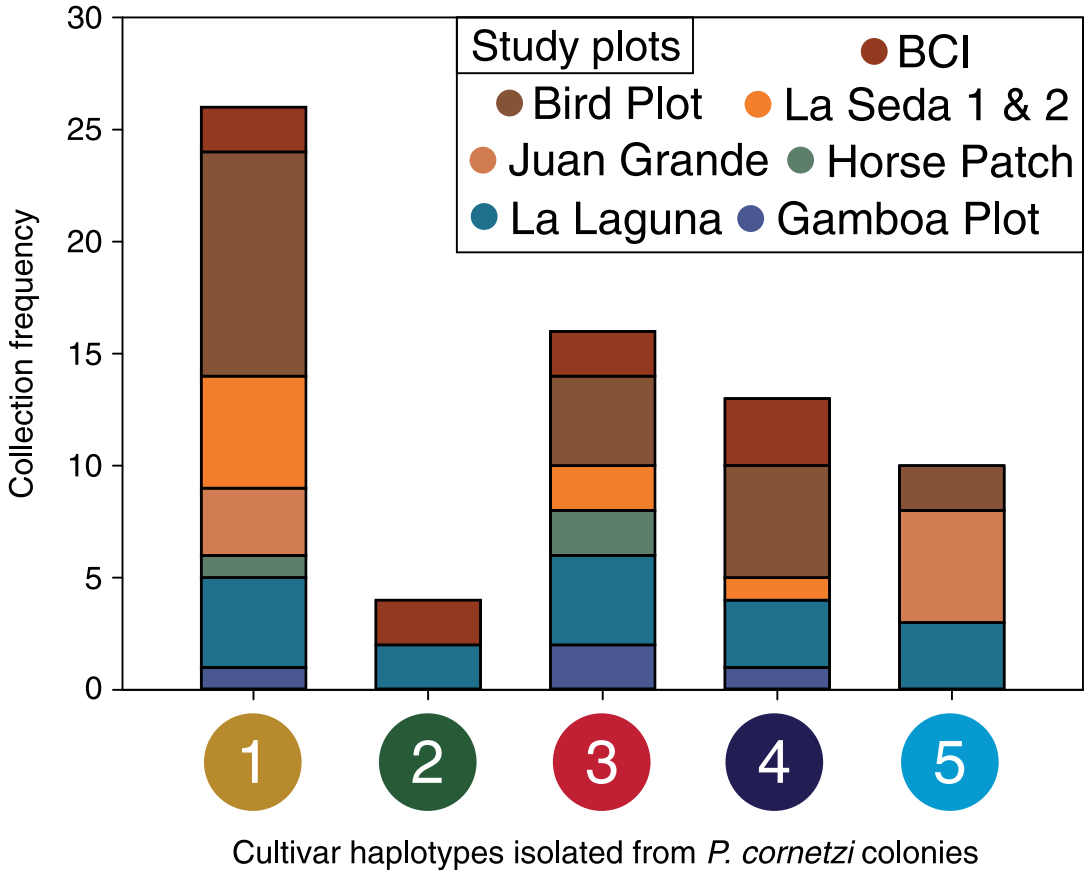

Extended Data Fig. 9 | Each of the five fungal haplotypes cultivated by P. cornetzi was widely distributed across Soberanía National Park. For a map of these sampling locations, see Extended Data Fig. 10, Supplementary Table 14. We combined cultivars from La Seda plots 1 and 2 for this figure since these plots were within 200 m of each other. Four of the five fungal haplotypes that we obtained from these Panama study plots matched cultivar haplotypes sampled from Brazilian colonies of *Paratrachymyrmex* and *Sericomyrmex* by Solomon et al.[35], suggesting broad geographic distributions extending across Central and South America. Additional Soberanía Park sampling localities where no specific plots were assigned (so no labels in Extended Data Fig. 10) included La Laguna (N 9.1196, W −79.6942), Horse Patch (N 9.11990, W −79.70730), and Barro Colorado Island (BCI: N 9.15744, W −79.83523).

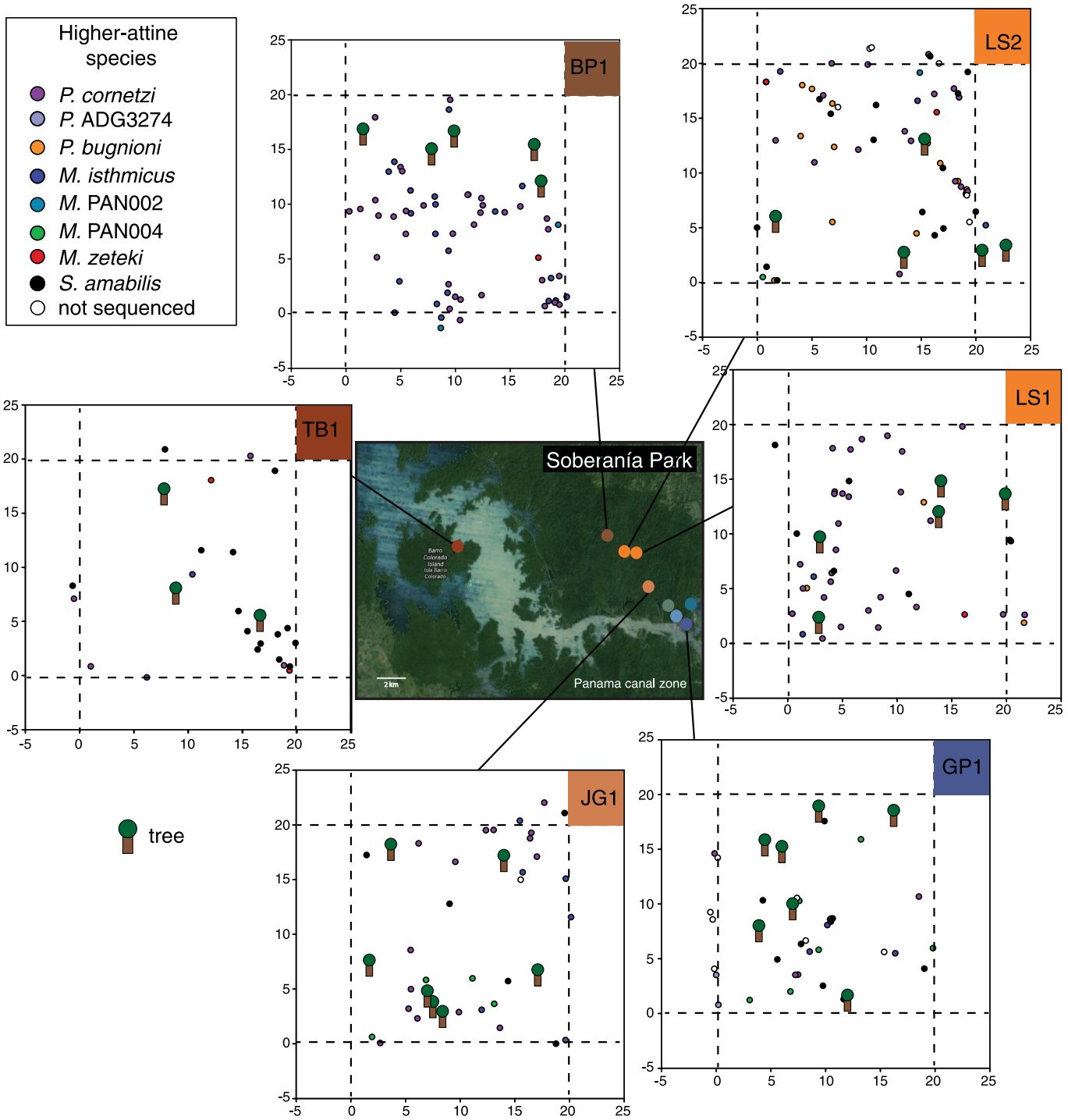

Extended Data Fig. 10 | We mapped local-scale higher neoattine colony distributions within the six 20-m² study plots distributed across Soberanía National Park. This totalled 263 colonies (9 species) that were mapped by tracking foraging workers back to their nests after which pinned specimens were screened in microsatellite (Extended Data Fig. 7) DNA barcoding analyses (Extended Data Fig. 8, Supplementary Table 13), as well as with morphological identification. We located colonies by placing bait (polenta) in the leaf litter and observing foragers for 27 ± 3 searching hours per plot (N = 163 total searching hours). The ant *M. opulentus* was recorded within the forest, but not within any of the 20 m² plots. Nests were marked by flags at nest entrances, which are inconspicuous holes under the leaf litter the circumference of a pencil. Within 20-m² plots, we observed 43 ± 17 (range: 21–66) higher-neoattine colonies representing 5 ± 1 (range: 4–7) higher-neoattine species. Dashed lines indicate boundaries of 20m² plots, and an additional 5 m is provided because some colonies were marked despite occurring just beyond the 20-m² plot border lines. Trees > 1 m circumference dbh were also mapped. Plot abbreviations were as follows: BP1: Bird Plot [N 9.16324, W −79.74553], GP1: Gamboa Plot [N 9.11489, W −79.69784], JG1: Juan Grande [N 9.13528, W −79.72141], LS1: La Seda [N 9.15451, W −79.73583], LS2: La Seda [N 9.15624, W −79.73472], TB1: Thomas Barbour [N 9.15744; W −79.83523]). The satellite image of the Panama Canal Zone is from Google Maps (credit to the images data supplier's used in the satellite image (Billeder © CNES / Airbus, Landsat / Copernicus, Maxar Technologies, U.S. Geological Survey, Kortdata © 2020)).

nature research

Corresponding author(s): Jonathan Z. Shik

Last updated by author(s): Aug 4, 2020

Reporting Summary

Nature Research wishes to improve the reproducibility of the work that we publish. This form provides structure for consistency and transparency in reporting. For further information on Nature Research policies, see our Editorial Policies and the Editorial Policy Checklist.

Statistics

For all statistical analyses, confirm that the following items are present in the figure legend, table legend, main text, or Methods section.

n/a	Confirmed	
☐	☒	The exact sample size (*n*) for each experimental group/condition, given as a discrete number and unit of measurement
☐	☒	A statement on whether measurements were taken from distinct samples or whether the same sample was measured repeatedly
☐	☒	The statistical test(s) used AND whether they are one- or two-sided *Only common tests should be described solely by name; describe more complex techniques in the Methods section.*
☐	☒	A description of all covariates tested
☐	☒	A description of any assumptions or corrections, such as tests of normality and adjustment for multiple comparisons
☐	☒	A full description of the statistical parameters including central tendency (e.g. means) or other basic estimates (e.g. regression coefficient) AND variation (e.g. standard deviation) or associated estimates of uncertainty (e.g. confidence intervals)
☐	☒	For null hypothesis testing, the test statistic (e.g. *F*, *t*, *r*) with confidence intervals, effect sizes, degrees of freedom and *P* value noted *Give P values as exact values whenever suitable.*
☐	☒	For Bayesian analysis, information on the choice of priors and Markov chain Monte Carlo settings
☒	☐	For hierarchical and complex designs, identification of the appropriate level for tests and full reporting of outcomes
☒	☐	Estimates of effect sizes (e.g. Cohen's *d*, Pearson's *r*), indicating how they were calculated

Our web collection on statistics for biologists contains articles on many of the points above.

Software and code

Policy information about availability of computer code

Data collection

We used the program ImageJ (NIH Image; V 1.49) to estimate fungal area from photographs of cultivars grown in vitro. We otherwise used standard empirical tools to collect data (e.g. a microbalance, Flash EA1112 analyser (CE Elantech, New Jersey, USA to measure elemental carbon (%C) and nitrogen (%N), etc.).

Data analysis

We used the following programs to analyse and visualize data:

1) Phylogenetic analysis of cultivar growth rate: To structure the analyses, we used the barcoding DNA sequences to generate a pruned chronogram by iterative alignment, simultaneously aligning and estimating the tree using SATé-II v 2.2.2. Before estimating the tree, we used jModelTest v 0.1.1 to determine the molecular model of the aligned sequences, and then selected the best fitting model for phylogenetic analyses. We then used Garli v 2.0 and MrBayes v 3.4 to perform a maximum likelihood (ML) and a Bayesian estimation (with default settings for all priors) of the phylogeny. Following this, we ran a Markov Chain Monte Carlo (MCMC) analysis six times independently with each run containing two chains of 75 million generations using a sampling rate of 1,500 generations after which we used convergence of runs was determined by Tracer v 1.4.

2) Microsatellite analyses: Data were analysed using STRUCTURE 2.3.4. The most likely subdivision for each analysis was determined by considering the second-order rate of change in log-likelihood of K (ΔK) using the R (V 3.2.4) package pophelper, which was also used to visualize the results.

3) Visualizing fungal cultivar FNNs: We mapped fungal growth areas and staphyla densities across the 36-diet arrays using the fields package in R (3.2.4). We plotted nutritional landscape contours using non-parametric thin-plate splines and set the topological resolution of response surfaces to λ = 0.001 as a smoothing parameter. We did the same for cultivar survival, but used a smoothing parameter of 0.01. We then used least-square regressions to assess the underlying significance of both linear and quadratic terms (and their interactions) and to verify the interpretation of FNN heatmaps based on fungal growth areas across the 36 protein and carbohydrate diet combinations.

4) Colony feeding experiment analyses: We performed the following statistical analyses in R (3.2.4) exploring P:C diet treatment effects on colony behaviour and performance separately for the three ant species. We first used general linear models to test for diet treatment effects on the response variables total macronutrients used, protein used, and carbohydrate used with initial worker number as a covariate. These data were log-transformed prior to analyses to meet the assumptions of normality and homoscedasticity. We also performed a survival analysis (survfit, ggsurvplot) in R (3.2.4) using a Cox proportional hazards model to test for diet treatment effects on crop failure in P. cornetzi, including initial fungus garden mass as a covariate. To further explore the links between foraging behaviour and colony demography in both P. cornetzi and A. colombica, we used GLM analyses to test for effects of P:C macronutrient mixes on changes in worker number and colony mass, analysing the slopes of linear regressions for each colony from values on day 1 to values on the final day of the experiment (day 39 in P. cornetzi, day 15 A. colombica) or on the day the colony was removed from the experiment due to crop failure (a subset of P. cornetzi colonies).

5) Nutritional analyses of foraged substrates: We used Near Infrared Spectrometry (NIRS) to estimate the nutritional composition of field-collected substrates harvested by leafcutter ants. We analyzed NIRS spectra of these 87 samples using Principal Component Analysis (PCA) with a 1st derivative model to select a subset of samples for chemical analysis using SIMCA software (Umetrics).

For manuscripts utilizing custom algorithms or software that are central to the research but not yet described in published literature, software must be made available to editors and reviewers. We strongly encourage code deposition in a community repository (e.g. GitHub). See the Nature Research guidelines for submitting code & software for further information.

Data

Policy information about availability of data

All manuscripts must include a data availability statement. This statement should provide the following information, where applicable:

- Accession codes, unique identifiers, or web links for publicly available datasets
- A list of figures that have associated raw data
- A description of any restrictions on data availability

The DNA sequences generated during this study are available at NCBI GenBank. This includes the data for: the 215 ant specimens (Accession codes for COI sequences provided in Supplementary Table 13), the 99 fungal cultivar samples (Accession codes for LSU and ITS sequences provided in Supplementary Table 14), and plant sample ITS1 sequences harvested by colonies of A. colombica (Accession codes provided in Supplementary Table 8). Ant sequence datasets and supporting information are also deposited in the Barcode of Life Data System70 (BOLD) under the project titled DS-ATTINENG "Nutritional niches reveal fundamental domestication tradeoffs in fungus-farming ants" (dx.doi.org/10.5883/DS-ATTINENG).

Field-specific reporting

Please select the one below that is the best fit for your research. If you are not sure, read the appropriate sections before making your selection.

☐ Life sciences ☐ Behavioural & social sciences ☒ Ecological, evolutionary & environmental sciences

For a reference copy of the document with all sections, see nature.com/documents/nr-reporting-summary-flat.pdf

Ecological, evolutionary & environmental sciences study design

All studies must disclose on these points even when the disclosure is negative.

Study description	The study had three types of related data collection: 1) in vitro studies of fungal performance on nutritionally defined media, 2) laboratory studies of fungus-growing ant colonies measuring performance when confined to nutritionally defined substrates, and 3) field studies of colony distributions, foraging behavior, and genetic diversity. I provide the detailed methods with sample sizes in the sections below (and where relevant throughout the manuscript). The research took place in a Panamanian tropical rainforest and many of the experiments and analyses took place at the Smithsonian Tropical Research Institute in Panama and at the home university in Denmark.
Research sample	Samples were whole attine colonies, fungal samples extracted from attine colonies (for culturing and molecular analyses), ant workers extracted from attine colonies (for molecular analyses), and substrates collected from mandibles of foraging ants in the field. For maps of colony distributions, samples were 20 m2 monitoring plots (n = 6) established throughout the 54 km2 Soberania Park in Panama.
Sampling strategy	Sampling strategies are described as follows: 1) In vitro fungal experiments: [we replicated within and across colonies as much as possible, within contraints imposed by species rarity and time in the field, and guided by similar published comparative studies in the literature]: We isolated fungus from 51 colonies of 10 attine species, including Mycocepurus smithii (10 colonies), Apterostigma dentigerum (3), Cyphomyrmex rimosus (1), C. costatus (3), C. longiscapus (1), Paratrachymyrmex cornetzi (13), Mycetomoellerius zeteki (2), Sericomyrmex amabilis (2), Acromyrmex echinatior (3), and Atta colombica (13). This represents the largest and most phylogenetically comprehensive comparative study of its type. We cultured these fungal cultivars on sealed sterile petri dishes containing PDA media (potato dextrose agar, DIFCO) and used them to generate pure fungal stock cultures. We then used PDA as a standard medium to compare cultivar growth rates placing 19.6 mm2 cylindrical plugs of pure culture into separate 60 x 15 mm petri dishes containing 15 ml of PDA. To estimate these intrinsic growth rates, we photographed the plates every 10 days for periods of 25 to 76 days (depending on the overall growth rate of the cultivar), and then used ImageJ (NIH Image; V 1.49) to measure cumulative fungal growth after 30 days (area mm2). Sample sizes are provided in Table S3. In a few cases, replicate sample sizes for a given cultivar were small due to loss of petri dishes to contamination (Table S3). But, in these cases, we replicated across colonies to ensure robust results. We also visualized the fundamental nutritional niches (FNNs) of cultivar fungi isolated from the nests of 10 attine species (N = 22 colonies), including M. smithii (1), Apterostigma dentigerum (3), Cyphomyrmex rimosus (1), C. costatus (3), C. longiscapus (1), P.

cornetzi (3), M. zeteki (2), Sericomyrmex amabilis (2), Acromyrmex echinatior (3), and A. colombica (3). For these experiments, we inoculated fungi in petri dishes containing 12 mL of 36 sterile synthetic agar-based 'diet' treatments varying in P:C (1:9, 1:6, 1:3, 1:2, 1:1, 2:1, 3:1, 6:1, 9:1) and P + C concentration (8g/L, 20g/L, 40g/L, 60g/L) (n = 8 plates per diet x dilution treatment, N = 288 plates per colony, N = 6,336 plates).

2) Colony feeding experiments: We used published examples of colony-level replication as guidance for sample sizes. We also tailored experimental protocols to fit the different foraging rates and farming scales of each species, replacing diets every day for A. colombica (n = 5 colonies per diet treatment, N = 25) and M. smithii (n = 5 colonies per diet treatment (N = 25), or every second day for P. cornetzi (n = 10 colonies per diet treatment; N = 50). For M. smithii, some of the colonies were subsampled from larger colonies (see published paper by Shik et al. (2016). We used colony ID as a random factor where relevant for all analyses related to this species. We sampled (and barcoded workers) P. cornetzi and A. colombica to ensure that each colony was a distinct colony.

3) Field research:
A) Collecting substrates from ant mandibles: We collected substrate carried by laden workers returning to nests of 49 mapped P. cornetzi colonies from 8AM to 4PM during ~1-hour observation periods (43.7 total hours) in the wet season (Nov 16 to Dec 31 in 2013 and Jan 2 to Jan 17 in 2014) (raw data provided in Table S7). The substrates collected by M. smithii were obtained using the same protocols, as described in the Shik et al. (2016) paper. During observation periods, we lay on trash bags next to nest entrances using a headlamp to maximize visibility and carefully grabbed laden foragers with forceps just before they disappeared underground. We collected these substrate pieces in Eppendorf tubes and then dried them at 60°C for 24 hours before classifying them into six categories: insect frass, leaf fragment, wood, flower, seed, and other (miscellaneous plant, insect piece, unknown), and weighing them to the nearest 1 µg on a Sartorius CP2P microbalance. We then calculated the fraction of biomass of each substrate type relative to the total biomass of substrate collected. The much larger quantities of fresh vegetative substrates harvested by leafcutter ants required different collection methods and also facilitated more detailed nutritional analyses. In May 2019 (the wet season, a period of high ant activity at the BCNM), we located an A. colombica colony at La Laguna (W 9.11672, N -79.69514) as part of a larger unpublished study on Atta foraging ecology. We laid down on trash bags next to the most active trail, close to the nest entrance and hand-collected a total of 6,868 fragments (40,026 mg dry mass) carried by laden foragers during 3 periods of 1.5 hours (4.5 hours in total) between 9AM and 12AM (raw data provided in Table S8).

B) Measuring attine ant and cultivar diversity: The single species status of A. colombica and its fungal cultivar L. gongylophorus in central Panama are not in question and the same applies for M. smithii except that this basal attine ant is known to be associated with a series of fungal cultivars, that were recognized in our previous study of the nutritional geometry of this species. However, this is much more ambiguous for P. cornetzi and their fungal symbionts, because a previous small-scale study showed that there is substantial cryptic diversity not only among the cultivars but also among the ants. To avoid biased interpretations of our present results due to overlooking (and unjustifiably pooling) cryptic species of farming ants and cultivars, we did an extensive survey across a large meta-population of P. cornetzi (54 km2 of Soberanía Park forest) and within the local populations represented by our six 20m2 plots (plot distributions visualized in Fig. S13). Within these study plots, we mapped all higher-attine nests by dispersing oat-polenta bait in the leaf litter and following laden workers back to their nests (N = 263 nests across all plots, n = 27 ± 3 searching hours per plot). From each nest, we then collected 2-4 workers in vials with 95% ethanol while also sampling workers from 85 additional Paratrachymyrmex and Mycteomoellerius colonies distributed across Soberanía Park (N = 297 colonies across these two genera). We similarly sampled 30 A. colombica colonies distributed across the Gamboa area. We then identified the ant (morpho)species using morphological analysis of vouchers, as well as analysis of DNA microsatellite markers and mtDNA barcoding.
We used DNA microsatellite analyses to examine the nuclear gene population structure of workers from 28 A. colombica colonies (Structure plot in Fig. S11) and 297 Paratrachymyrmex and Mycetomoellerius colonies (Structure plot in Fig. S11) using a total of nine highly variable markers (Ant7680, Ant859, Ant1343, Ant2341, Ant3993, Ant11400, Ant3653, Ant4155, Ant8498). To supplement our nuclear microsatellite data, we also used mtDNA barcoding analyses of a mitochondrial marker, which included 147 Paratrachymyrmex, 38 Mycetomoellerius colonies and 29 A. colombica colonies. A subset of these ants was paired with their fungal cultivars to examine farmer-cultivar association patterns, as we excavated 69 colonies of putative P. cornetzi (21 January to 25 February 2014) and 29 colonies of A. colombica (16 to 30 June 2014). For each of these colonies we collected a clean 2-cm3 fraction of fungus garden with forceps into vials with 95% ethanol soon after excavation.

Data collection

Data was collected by the following co-authors:

1) In vitro fungal performance: Ernesto Gomez, Mariana Franco, Jonathan Shik:
We cultured these ant cultivars on sealed sterile petri dishes containing PDA media (potato dextrose agar, DIFCO) and used them to generate pure fungal stock cultures. We then used PDA as a standard medium to compare cultivar growth rates placing 19.6 mm2 cylindrical plugs of pure culture into separate 60 x 15 mm petri dishes containing 15 ml of PDA. To estimate these growth rates, we photographed the plates every 10 days for periods of 25 to 76 days (depending on the overall growth rate of the cultivar; raw data in Table S3), and then used ImageJ (NIH Image; V 1.49) to measure cumulative fungal growth after 30 days (area mm2).

To measure cultivar FNNs, we inoculated fungi in petri dishes containing 12 mL of 36 sterile synthetic agar-based 'diet' treatments varying in P:C (1:9, 1:6, 1:3, 1:2, 1:1, 2:1, 3:1, 6:1, 9:1) and P + C concentration (8g/L, 20g/L, 40g/L, 60g/L) (n = 8 plates per diet x dilution treatment, N = 288 plates per colony, N = 6,336 plates). We used growth rates on standard PDA media to set the length of P:C growth experiments for each cultivar. Nutritionally defined cultivar substrates included distilled water and bacteriological agar (1.6% w:v; Amresco, Inc.), carbohydrates as equal parts sucrose (Doradita ® cane sugar) and starch (puriss p.a., from potato, reag. ISO, Sigma-Aldrich), and protein as equal parts bacto-peptone (enzymatic digest of protein, Becton, Dickinson and Company), trypticase peptone (pancreatic digest of casein, BD), and bacto tryptone (pancreatic digest of casein, BD). We also included a crushed multivitamin mixture (Centrum ®) at a concentration of 2% of the mass of protein + carbohydrates. Recipes provided in Shik et al. (2016). These ingredients were mixed with 200 ml distilled water on a stirring plate for 5 minutes and then sterilized by autoclaving at 121°C, yielding a pH of 6.9. Each of the higher-attine and leafcutter cultivar haplotypes that we tested exhibited mortality on a subset of P:C diets outside the range of the FNN. Mortality was indicated by inoculation plugs being clear (empty of fungus) or by lack of growth from the inoculation plug onto the P:C diet by the end of the experiment (Results provided in Fig. S2).

2) Colony feeding experiments: Ernesto Gomez, Jonathan Shik, Xavier Arnan
We analysed nutrient regulation strategies of lab-acclimated colonies using nutritional geometry feeding experiments, based on agar-based mixtures of protein and carbohydrate macronutrients (1.6g agar/L) at P:C ratios of 1:6, 1:3, 1:1, 3:1, and 6:1, and protein + carbohydrates dilutions of 100 g/L (for P. cornetzi and A. colombica) (Table S10) or 20 g/L (for M. smithii). In these no-choice

experiments, we confined colonies to a single P:C diet for 29 days (M. smithii), 39 days (P. cornetzi), or 15 days (A. colombica). We tailored experimental protocols to fit the different foraging rates and farming scales of each species, replacing diets every day for A. colombica (n = 5 colonies per diet treatment, N = 25) and M. smithii (n = 5 colonies per diet treatment (N = 25), or every second day for P. cornetzi (n = 10 colonies per diet treatment; N = 50). We provide raw pre- and post-experiment colony demography data for colonies in Table S5.

We calculated protein and carbohydrate use by the ants from the agar P:C ratios and diet dry mass loss estimated from dry:wet mass ratios of control agar fragments for each P:C ratio (as in previously published papers). We weighed colonies on the first (initial colony mass) and last day (final colony mass) of the experiments, and calculated worker mortality rates by matching the collecting dead workers each time we changed diets. During the M. smithii and P. cornetzi experiments, a number of colonies showed signs of crop failure (i.e., elevated worker mortality, living workers ceasing foraging and discarding fungus garden material). For our demographic analyses, we assessed crops as having failed on the day colonies no longer had any fungus garden biomass left.
We did not analyse treatment effects on brood production, since it was difficult to safely measure initial brood demography (brood were embedded within fungus gardens), and because experiments were designed to assess worker provisioning responses to nutritionally defined agar mixtures rather than a colony's ability to rear new workers over multiple egg-to-adult intervals. We additionally note that queens were not found in 5 of 50 colonies of P. cornetzi (1:3 (1), 1:6 (2), 3:1 (2)) and 3 of 25 colonies of A. colombica (1:3 (1), 1:6 (1), 3:1 (1)) when they were disassembled for demographic analyses following feeding experiments. While it was not possible to assess queen presence initially, given that they are usually in the centre of the fungus garden and searching for them causes substantial disturbance to the colony, this factor did not impact the statistical results so the reported results include these queenless colonies.

3) Field work and molecular/phylogenetic analyses: Jonathan Shik, Ernesto Gomez, David Donoso, Pepijn Kooij, Juan Santos, Jack Howe, Antonin Crumiere

A) Colony location/collection/mapping [Shik, Gomez], Donoso, Kooij]: All attine colonies were harvested from the lowland tropical rainforest at Soberanía National Park, Panamá (N 9.13528, W 79.72141) from 28 October 2013 to 10 June 2015, with additional fieldwork conducted from 1 May to 30 June 2019 (more detail provided in "Timing and Spatial Scale" section below).

B) Substrate collection from worker mandibles [Shik, Gomez, Crumiere]: We collected substrate carried by laden workers returning to nests of 49 mapped P. cornetzi colonies from 8AM to 4PM during ~1-hour observation periods (43.7 total hours) in the wet season (Nov 16 to Dec 31 in 2013 and Jan 2 to Jan 17 in 2014) (raw data in Table S7). The substrates collected by M. smithii were obtained using the same protocols, as described in Shik et al. (2016). During observation periods, we lay on trash bags next to nest entrances using a headlamp to maximize visibility and carefully grabbed laden foragers with forceps just before they disappeared underground. We collected these substrate pieces in Eppendorf tubes and then dried them at 60°C for 24 hours before classifying them into six categories: insect frass, leaf fragment, wood, flower, seed, and other (miscellaneous plant, insect piece, unknown), and weighing them to the nearest 1 µg on a Sartorius CP2P microbalance. We then calculated the fraction of biomass of each substrate type relative to the total biomass of substrate collected.
We homogenized a subset of these dried substrate categories and determined their elemental carbon (%C) and nitrogen (%N) in the lab of Ben Turner (Smithsonian Tropical Research Institute, Panama) with a Flash EA1112 analyser (CE Elantech, New Jersey, USA). The small size of these substrate fragments precluded direct macronutrient-level analyses of their % protein and % carbohydrates. To acquire these estimates, in June 2019, we used 30 1-m2 tarps placed on leaf litter for 24-hour intervals to collected a large amount of frass that fell from the canopy in the same forests. Back in Copenhagen, we created a 1 g pooled frass sample which we freeze-dried (using a SP Scientific BenchTop Pro with Omnitronics) for 24 hours, homogenized and analysed for %C (Eurovector CN analyser coupled to an Isoprime isotope ratio mass spectrometer in the lab of Anders Michelsen, University of Copenhagen), as well as total non-structural carbohydrates (TNC: water soluble carbohydrates + starch). Using the wet chemistry approaches of Felton et al. (2009), we analysed 25 mg of frass with a Total Carbohydrate Assay Kit (Sigma-Aldrich) to determine water soluble carbohydrates, and 50 mg of frass with a Total Starch Assay Kit (Megazyme) to quantify starch. We used 5 replicates for each quantification. We used these data to convert %C to %TNC in the frass and tiny wood fragments (2.59%) in the existing dataset. To estimate % TNC in the three flower fragments harvested by P. cornetzi, we removed 17% from each %C value, roughly corresponding to the amount of cellulose in a typical leaf62. From the elemental N data, we estimated crude protein (i.e. including non-available protein bound up by tannins) by multiplying substrate N mass by the standard conversion factor 6.256.
The much larger quantities of fresh vegetative substrates harvested by leafcutter ants required different collection methods and also facilitated more detailed nutritional analyses. In May 2019 (the wet season, a period of high ant activity at the BCNM), we located an A. colombica colony at La Laguna (W 9.11672, N -79.69514) and laid down on trash bags next to the most active trail, close to the nest entrance. We hand-collected a total of 6,868 fragments (40,026 mg dry mass) carried by laden foragers during 3 periods of 1.5 hours (4.5 hours in total) between 9AM and 12AM (raw data in Table S8). These fragments (almost all fresh plant material) were stored into new Ziplock bags every 30 minutes that were promptly transferred to a cooler. Back in the lab, we catalogued the forage fragment samples under a microscope based on the morphology of the veins of leaf fragments, weighed the specific fractions and freeze-dried for 24 hours as described above. We then stored the samples at -20C in new Ziploc bags with silica gel until subsequent nutrient analysis.
We homogenized a subset of these dried substrates into powder and used near infrared reflectance spectroscopy (NIRS) to estimate the concentrations of total nitrogen, total protein, total non-structural carbohydrate, and starch in all 17 categories of plant substrates sampled. We acquired NIRS reflectance spectra for each sample using an Antaris II FT-NIR Analyzer (Thermo Scientific) from 4.000 to 10.000 cm-1 (2.500 to 1.000 nm) at a resolution of 16 cm-1 and 2x gain. We used the standard default reference within the instrument to calibrate each measurement. For each sample, 32 monochromatic scans were acquired to calculate the average value. We performed three acquisitions per samples as technical replicates and then calculated an average value.
The NIRS spectra of these 17 samples were interpreted based on additional scans of 70 other harvested leaf species as part of a larger study on leafcutter ant ecology involving 6 different colonies across the area (unpublished). We used an Eurovector CN analyser (Pavia, Italy) coupled to an Isoprime isotope ratio mass spectrometer to quantify total nitrogen from 3-4 mg of homogenized samples (A. Michelsen lab, University of Copenhagen). We estimated crude total protein content as before by multiplying total N by 6.25. We quantified water soluble carbohydrates with a Total Carbohydrate Assay Kit (Sigma-Aldrich) and 25 mg homogenized material and starch with a Total Starch Assay Kit (Megazyme) and 50 mg of homogenized material. We used these data to build predictive models of the concentration of total protein and total non-structural carbohydrates in our 17 samples using 1st derivative model with SIMCA software (Umetrics). The predictive models were validated by cross-validation with a 500 permutation parameter. Characteristics for predictive models are described in Table S11.

C) Colony mapping [Shik, Gomez]:
Within these study plots, we mapped all higher-attine nests by dispersing oat-polenta bait in the leaf litter and following laden workers back to their nests (N = 263 nests across all plots, n = 27 ± 3 searching hours per plot). From each nest, we then collected 2-4 workers in vials with 95% ethanol (for molecular analyses) while also sampling workers from 85 additional Paratrachymyrmex and Mycteomoellerius colonies distributed across Soberanía Park (N = 297 colonies across these two genera). We similarly sampled 30 A. colombica colonies distributed across the Gamboa area.

D) Microsatellite analyses [Shik, Howe, Kooij]: We used DNA microsatellite analyses to examine the nuclear gene population structure of workers from 28 A. colombica colonies (Structure plot in Fig. S11) and 297 Paratrachymyrmex and Mycetomoellerius colonies (Fig. S11) using a total of nine highly variable markers (Ant7680, Ant859, Ant1343, Ant2341, Ant3993, Ant11400, Ant3653, Ant4155, Ant8498)66. Based on the retrospective partitioning of the material, colony-level sample sizes for the ant species included in this analysis were: P. cornetzi, n = 157; P. ADG3274, n = 16; P. bugnioni, n = 21; M. isthmicus, n = 36; M. opulentus, n = 3; M. PAN002, n = 34; M. PAN004, n = 17; M. zeteki, n = 13). Microsatellite markers were analyzed using PCR with 5 µl VWR Red Taq DNA polymerase Master Mix (VWR International, Haasrode, Belgium), 0.1 µl 10µM forward and reverse primer each, 3.8 µl ddH2O and 1 µl DNA, and a program of 10 minutes denaturing at 95C, followed by 40 cycles of 15 seconds denaturing at 95C, 30 seconds annealing at 55C and 30 seconds extension at 72C, and finally a 10 min extension at 72C. Microsatellite amplification products were analyzed on an ABI PRISM 3730 automated DNA sequencer (PerkinElmer, Applied Biosystems). Specific allele scorings were obtained by analysing chromatograms in Genemapper 5.0 (Applied Biosystems).
Microsatellite data were analysed using STRUCTURE 2.3.4. We conducted a STRUCTURE analyses for Paratrachymyrmex and Mycetomoellerius and a separate STRUCTURE analysis for the Atta samples, probing the fit of a range of possible population subdivisions (Atta: K=1-5; Paratrachymyrmex + Mycetomoellerius: K=1-12), always with 25 iterations per K-value. The Paratrachymyrmex-Mycetomoellerius analyses comprised a burn-in of 200,000 and 5,000,000 MCMC repetitions, whereas analyses for Atta had a burn-in of 100,000 and 2,000,000 MCMC repetitions. The most likely subdivision for each analysis was determined by considering the second-order rate of change in log-likelihood of K (ΔK)68 using the R package pophelper, which was also used to visualize the results. As the results of our Paratrachymyrmex-Mycetomoellerius analyses implied potential nested subdivisions within the data, we ran three stages of analyses, testing for population structure within: 1) the entire data set (K=1-12), 2) only P. cornetzi (K=1-6), and 3) all data minus those of P. cornetzi (K=5-11).

E) mtDNA barcoding analyses [Shik, Kooij, Donoso, Santos]:
We used DNA barcoding analyses of a mitochondrial marker, which included 147 Paratrachymyrmex, 38 Mycetomoellerius colonies and 29 A. colombica colonies. A subset of these ants was paired with their fungal cultivars to examine farmer-cultivar association patterns, as we excavated 69 colonies of putative P. cornetzi (21 January to 25 February 2014) and 29 colonies of A. colombica (16 to 30 June 2014). For each of these colonies we collected a clean 2-cm3 fraction of fungus garden with forceps into vials with 95% ethanol soon after excavation. Mitochondrial DNA from ant workers was obtained with 10% Chelex extractions70 followed by PCR amplification of ~1100 bp of the Cytochrome Oxidase 1 gene using a combination of the universal arthropod primers for two overlapping regions: Lep-F171 (5'-ATTCAACCAATCATAAAGATAT-3') and Lep-R171 (5'-TAAACTTCTGGATGTCCAAAAA-3'), and Jerry72 (5'-CAACATTTATTTTGATTTTTTGG-3') and Ben73 (5'-GCWACWACRTAATAKGTATCATG-3'. Samples where boiled at 99°C for 1hr in 150µL 10% Chelex X-100 (Sigma) and stored in the freezer for further analyses. DNA from fungal cultivars was obtained with 10% Chelex extractions70 followed by PCR amplification of the nuclear large subunit rRNA (LSU) [~820 b.p.] and the Internal Transcribed Spacer unit (ITS) [~550 b.p.]. For LSU, we used the universal primers LR0R74 (5'-ACCCGCTGAACTTAAGC-3') and LR575 (5'-TCCTGAGGGAAACTTCG-3') and for ITS the primers ITS1-F76 (5'-CTTGGTCATTTAGAGGAAGTAA-3') and ITS4-B76 (5'-CAGGAGACTTGTACACGGTCCAG-3'). Amplification was performed with PCR with 5µL DreamTaq PCR Master Mix (Thermo Scientific), 0.2µL 10µM forward and reverse primer each, 2µL TBT-PAR 5x, 1.6µL ddH2O and 1µL DNA, and a program of 4 minutes denaturing at 94C, followed by 36 cycles of 30 seconds denaturing at 94C, 45 seconds annealing at 53C, and 1 minute and 30 seconds extension at 72C, and finally a 10 minutes extension at 72C, for both LSU and ITS.
For COI (Ben-Jerry), amplification was performed with PCR with 5µL VWR Red Taq DNA polymerase Master Mix (VWR International, Haasrode, Belgium), 0.2µL 10µM forward and reverse primer each, 0.2µL 25mM MgCl2, 3.4µL ddH2O and 1µL DNA, and a program of 5 minutes denaturing at 95C, followed by 25 cycles of 30 seconds denaturing at 95C, 45 seconds annealing at 60-55C with a touchdown of -0.2C per cycle, and 1 minute extension at 72C, followed by 20 cycles of 30 seconds denaturing at 95C, 45 seconds annealing at 55C, and 1 minute extension at 72C, and finally a 10 minutes extension at 72C.
For COI (Lep), amplification was performed with PCR with 10µL VWR Red Taq DNA polymerase Master Mix (VWR International, Haasrode, Belgium), 0.5µL 10µM forward and reverse primer each, 0.4µL 25mM MgCl2, 7.6µL ddH2O and 1µL DNA, and a program of 1 minute denaturing at 94C, followed by 6 cycles of 1 minute denaturing at 94C, 1 minute and 30 seconds annealing at 45C, and 1 minute and 15 seconds extension at 72C, followed by 36 cycles of 1 minute denaturing at 94C, 1 minute and 30 seconds annealing at 51C, and 1 minute and 15 seconds extension at 72C, and finally a 5 minutes extension at 72C.
PCR products were cleaned up using an enzymatic purification by adding 0.4 times the PCR volume of 1:10 diluted ExoFAP (Exonuclease I [Fermentas, Waltham, MA USA]: FastAP Thermosensitive Alkaline Phosphatase [Fermentas, Waltham, MA USA] 1: 2). The cleaned-up PCR products were prepared for sequencing on an ABI PRISM 3730 by mixing 2µL of the PCR product to 0.2µL BigDye (Thermo Fisher Scientific), 1µL buffer (Thermo Fisher Scientific), 0.3µL 25mM MgCl2, 1.5µL ddH2O and 0.2µL 10µM primer, for each primer separately. Cycle sequencing then followed a program of 2 min denaturing at 95C, followed by 60 cycles of 10 sec denaturing at 95C, 10 sec annealing at 50C, and 2 min extension at 60C. Final products were cleaned-up through ethanol precipitation and sequenced on the ABI PRISM 3730 using standard protocols. The resulting sequences will be deposited in GenBank prior to manuscript publication.
To further interpret our molecular evidence confirming known species and detecting cryptic species among the collected P. cornetzi-like colonies within Soberanía Park, we also explored the biogeographic distribution of this species complex by comparing our sequence data to sequences of 8 Costa Rican ants and 1 Ecuadorian P. cornetzi ant specimen available on the Barcode of Life Data System.

Phylogenetic analyses [Juan Santos]:
We isolated cultivars from 13 colonies of P. cornetzi and 12 colonies of A. colombica and grew them on PDA medium for 40-70 days to measure intrinsic growth rate as described above. For P. cornetzi, we examined fungal haplotypes 1, 3 and 5, as fungal haplotypes 2 and 4 were no longer available. To structure the analyses, we used the barcoding DNA sequences to generate a pruned chronogram by iterative alignment, simultaneously aligning and estimating the tree using SATé-II v 2.2.278. Before estimating the tree, we used jModelTest v 0.1.1 to determine the molecular model of the aligned sequences, and then selected the best fitting model for phylogenetic analyses. We then used Garli v 2.0 and MrBayes v 3.4 to perform a maximum likelihood (ML) and a Bayesian estimation (with default settings for all priors) of the phylogeny. Following this, we ran a Markov Chain Monte Carlo (MCMC) analysis

six times independently with each run containing two chains of 75 million generations using a sampling rate of 1,500 generations after which we used convergence of runs was determined by Tracer v 1.4. For both the ML approach and the Bayesian posterior probability estimations we calculated nodal support after 200 nonparametric bootstrap searches, which yielded similar tree topologies. Only the ML phylogenies are provided.

Timing and spatial scale

All attine colonies were harvested from the lowland tropical rainforest at Soberanía National Park, Panamá (N 9.13528, W 79.72141) from 28 October 2013 to 10 June 2015, with additional fieldwork conducted from 1 May to 30 June 2019. We located nest entrances of lower and higher attines under leaf litter by placing polenta bait on the ground and following laden workers back to their nests. Leafcutter nests were visible as large established colonies and small dirt mounds of recently founded colonies. Back in the lab at the Smithsonian Tropical Research Institute in Gamboa, we established colonies in plastic containers with ad lib water and ground polenta (or leaves for Atta and Acromyrmex), and acclimated them to lab conditions at 24°C.

We collected substrate carried by laden workers returning to nests of 49 mapped P. cornetzi colonies from 8AM to 4PM during ~1-hour observation periods (43.7 total hours) in the wet season (Nov 16 to Dec 31 in 2013 and Jan 2 to Jan 17 in 2014) (raw data in Supplementary Tables 7-9). In May 2019 (the wet season, a period of high ant activity at the BCNM), we located an A. colombica colony at La Laguna (W 9.11672, N -79.69514) and laid down on trash bags next to the most active trail, close to the nest entrance. We hand-collected a total of 6,868 fragments (40,026 mg dry mass) carried by laden foragers during 3 periods of 1.5 hours (4.5 hours in total) between 9AM and 12AM (raw data in Table S8).

Data exclusions

We were careful when identifying colonies for inclusion in the colony feeding experiment--One colony from the P. cornetzi experiment (3:1_2 [176936]) was removed from the study since its fungus garden was lost before the start of the feeding experiment. Four additional putative P. cornetzi colonies were also removed from all subsequent analyses because barcoding and microsatellite analyses revealed they were actually the cryptic Paratrachymyrmex species P. ADG3724 (1:1_9 [177252], 1:1_8 [177340], 1:6_7 [177337], 1:6_8 [177352]), even though their exclusion did not change the results.

Reproducibility

1) In vitro fungal experiments: We replicated wherever possible within and across colonies. We based our approaches on established/published protocols within the field of Nutritional Geometry. We collected and cultured the fungi using established and published methods. In the main body of the manuscript and supplementary materials, we provide cultivar heatmaps (and statistical analyses based on means (across colonies) and for fungi isolated from each separate colony. We interpret clearly where the results were consistent and where variation occurred.

2) Colony feeding experiments: we replicated as much as was feasible across colonies within diet treatments. We compared our results to other published Nutritional Geometry ant colony feeding experiments and used versions of published diets. We have ample experience rearing attine colonies.

3) Field research: We collected a large dataset of ants and fungal cultivars and used mtDNA barcoding and microsatellite analyses to account for cryptic species diversity. We also replicated our colony mapping approach across six large 20m2 plots. We provide Lat-Long information for collection localities wherever appropriate.

Randomization

In the In vitro fungal experiments and colony feeding experiments, the experiments (including staphyla counting) were performed by two lab technicians unfamiliar with the theoretical implications of the results (Gomez and Franco). In the colony feeding experiment, we assigned colonies to diets to ensure there were no initial differences among diet treatments in colony mass for M. smithii ($F_{4,20} = 0.74$; $p = 0.58$), P. cornetzi ($F_{4,40} = 0.27$; $p = 0.90$), or A. colombica ($F_{4,20} = 0.12$; $p = 0.97$).

Blinding

Blinding was not relevant for this study.

Did the study involve field work? ☒ Yes ☐ No

Field work, collection and transport

Field conditions

All attine colonies were harvested from the lowland tropical rainforest at Soberanía National Park, Panamá (N 9.13528, W 79.72141) from 28 October 2013 to 10 June 2015, with additional fieldwork conducted from 1 May to 30 June 2019. Ants were observed during periods of peak seasonal (rainy season) and diurnal (ca. 9 AM to 12PM) activity. Conditions were typical of a seasonal wet tropical rainforest, and consistent with other published papers for the attine lineage.

Location

Soberanía National Park, Panamá (N 9.13528, W 79.72141). Elevation was near sea level.

Access & import/export

The Smithsonian Tropical Research Institute (STRI) provided support and use of facilities in Gamboa, and the Autoridad Nacional del Ambiente y el Mar (ANAM) gave permission to JJB and JZS to sample attines in Panama and export them to Denmark. Collection and export permits in Panama were renewed annually and were valid throughout the duration of this study.

Disturbance

There was only minimal disturbance from digging up some colonies. These collections were of species that were common to the study area and remained common during repeated subsequent site visits.

Reporting for specific materials, systems and methods

We require information from authors about some types of materials, experimental systems and methods used in many studies. Here, indicate whether each material, system or method listed is relevant to your study. If you are not sure if a list item applies to your research, read the appropriate section before selecting a response.

Materials & experimental systems

n/a	Involved in the study
☒	☐ Antibodies
☒	☐ Eukaryotic cell lines
☒	☐ Palaeontology and archaeology
☐	☒ Animals and other organisms
☒	☐ Human research participants
☒	☐ Clinical data
☒	☐ Dual use research of concern

Methods

n/a	Involved in the study
☒	☐ ChIP-seq
☒	☐ Flow cytometry
☒	☐ MRI-based neuroimaging

Animals and other organisms

Policy information about studies involving animals; ARRIVE guidelines recommended for reporting animal research

Laboratory animals	We brought some attine colonies into the lab for in vitro and whole colony nutritional experiments. This was sanctioned by collection/export permits: Mycocepurus smithii, Apterostigma dentigerum, Cyphomyrmex rimosus, C. costatus, C. longiscapus, Paratrachymyrmex cornetzi, Mycetomoellerius zeteki, Sericomyrmex amabilis, Acromyrmex echinatior, and Atta colombica.
Wild animals	These attine species were also studied in the field, in long-term established field sites in Panama.
Field-collected samples	We established attine colonies (M. smithii, P. cornetzi, A.colombica) in the lab at the Smithsonian Tropical Research Institute in Gamboa, we established colonies in plastic containers with ad lib water and ground polenta (or leaves for Atta and Acromyrmex), and acclimated them to lab conditions at 24°C, with ambient light conditions. We cultured fungi in petri dishes under these same environmental conditions, but in dark boxes.
Ethics oversight	No ethical approval was necessary.

Note that full information on the approval of the study protocol must also be provided in the manuscript.